

Article

Climate Change Effects upon Pasture in the Alps: The Case of Valtellina Valley, Italy

Francesca Casale *  and Daniele Bocchiola 

Department of Civil and Environmental Engineering, Politecnico di Milano, 20133 Milano, Italy

* Correspondence: francesca.casale@polimi.it; Tel.: +39-022-399-6210

Abstract: In this study, we assessed the potential effects of climate change upon the productivity of mountain pastures in the Valtellina valley of Italy. Two species, *Trisetum flavescens* and *Nardus stricta*, among the most abundant in Italian pastures, were chosen for the simulation of low- and high-altitude pastures, respectively. We introduced some agroclimatic indices, related to growing season parameters, climate, and water availability, to evaluate the impacts of climate change upon pasture production. First, the dynamic of the pasture species was evaluated for the present period using the climate-driven, hydrologically based model *Poli-Hydro*, nesting the *Poli-Pasture* module simulating plants growth. *Poli-Pasture* was validated against yield data, at province scale, and at local scale. Then, agroclimatic indices were calculated. Subsequently, IPCC scenarios of the Fifth and Sixth Assessment Reports (AR5 and AR6) were used to project species production and agroclimatic indices until the end of the 21st century. In response to increased temperature under all scenarios, a large potential for an increased growing season length and species yield overall (between +30% and +180% for AR5 at 2100) was found. Potential for decreased yield (until −31% for AR5) is seen below 1100 m asl in response to heat stress; however, it is compensated by a large increase higher up (between +50% and +140% for AR5 above 2000 m asl). Larger evapotranspiration is foreseen and larger water demand expected. However, specific (for hectares of pasture) water use would decrease visibly, and no significant water limitations would be seen. Results provide preliminary evidence of potential livestock, and thereby economic development in the valley at higher altitudes than now.



Citation: Casale, F.; Bocchiola, D. Climate Change Effects upon Pasture in the Alps: The Case of Valtellina Valley, Italy. *Climate* **2022**, *10*, 173. <https://doi.org/10.3390/cli10110173>

Academic Editors: Delle Rose Marco and Maria Teresa Caccamo

Received: 11 October 2022

Accepted: 4 November 2022

Published: 7 November 2022

Publisher's Note: MDPI stays neutral with regard to jurisdictional claims in published maps and institutional affiliations.



Copyright: © 2022 by the authors. Licensee MDPI, Basel, Switzerland. This article is an open access article distributed under the terms and conditions of the Creative Commons Attribution (CC BY) license (<https://creativecommons.org/licenses/by/4.0/>).

Keywords: agroclimatic indices; climate change; grasslands; hydrological modeling; Italian Alps; pasture modeling

1. Introduction

In mountain areas, pastures and farming systems are paramount important activities for local communities, a source of income for local development, and a key feature of local ecosystems dynamics [1]. Pasture management has positive effects on land sustainability, maintaining the landscape and cultural value and supporting biodiversity and soil fertility, thereby reducing soil loss and natural risks. On the contrary, land abandonment brings the growth of shrubs, grassland biodiversity loss, and increased erosion, wildfire, and avalanche risk, as well as the loss of traditional productive activities and typical landscapes [2]. During 1990–2010, ca. 17% of the Italian alpine pastures were abandoned [2].

In recent decades, climate change has had an impact on Alpine mountain ranges [3]. Already in the last 150 years, the temperature in the Alps increased by ca. +1.5 °C, higher than the global trend [4,5]. Atmospheric warming and changes in precipitation regimes shifted seasonal snow pack dynamics (with *high confidence* according to the IPCC Special Report on Cryosphere [3]) [6–10]. Warming may result in different evaporation rates, more erratic precipitation, increased frequency of floods, and droughts [11–16].

Projected trends until 2100 under the IPCC scenarios depict a large decrease in snowfall and snow cover during winter [9] (*high confidence* [3]), with ever earlier melting, larger

evapotranspiration from vegetation, and the subsequent loss of stream flows in warm seasons [17,18] (*high confidence* [3]).

Modified climate and hydrology at high altitudes may influence soil moisture, vegetation growth, and, in particular, pasture dynamics, which heavily depend upon temperature and precipitation. Snow cover extent and duration also affect pasture growing seasonality, area availability, and biomass [19,20].

An uplift of Alpine pasture species [5,21] is expected: species tends to adapt to higher altitudes, and this may cause a loss of pasture/grassland habitats at the lowest altitudes and habitat fragmentation [22,23].

Grassland dynamics in response to the climate can be modeled [24–26], and subsequently response to climate change assessed [27,28], thus giving a formal basis to correct adaptation plans of economic activities related to pasture areas.

Here, we report recent results in fulfilment of the IPCC MOUPA (*Interdisciplinary Project for assessing current and expected Climate Change impacts on MOUtain PASTures*) project. The primary goal of the present work was to evaluate the impact of climate change on grassland species commonly found in pastures of the Valtellina, an Alpine valley located in Northern Italy. In particular, we assessed climate change impacts on two species often found at low altitude (zone LowAlt) and high altitude (zone HighAlt) within the study area. To do so, we coupled *Poli-Hydro*, an already published hydrological model for the simulation of the hydrological cycle in high-altitude catchments [29], with *Poli-Pasture*, a degree-day model for simulating grassland species development [24], similar to the widely used *CropSyst* model [30]. We assessed climate change impacts by means of agroclimatic indices (henceforth AIs) available from literature [22,31–39]. We selected AIs related to climate, plant growth processes, and water resources availability, in particular AIs that highlight pressures experienced by the pastures over the growing season. AIs can be used to develop adaptation policies—namely to assess the overall impact of climate change—and anthropic use, and to monitor pasture performance [38–40]. Some of these AIs can be assessed using rapidly available (e.g., meteorological) data, while others need to be quantified using simulations of pasture growth and water use under given climate conditions. Few studies of pasture modeling in the Italian Alps are available [41,42], but usually pasture models do not specifically target the pasture dynamics in mountainous regions. Here, we developed a tool able to increase knowledge of pasture species growth and of climate change impacts therein in Italian alpine regions to aid the future management of pasture-related economic activities. Some points of novelty of our work with respect to former studies can be highlighted. As opposed to empirical, data-driven models, *Poli-Hydro* and *Poli-Pasture* are physically based, spatially distributed models, specifically developed for applications to high-altitude catchments. Here, a simulation of species dynamics for the entire Valtellina valley was pursued (covering more than 5000 km²), which is a step forward with respect to previous studies, which typically focus on a local (point) scale. Moreover, we innovatively investigated climate change impacts upon pastures, based upon the climate projections of the IPCC AR6. Valtellina valley has never been studied as a whole in terms of its pasture potential; thus, the results here are likely original and useful. Indeed, it is necessary to evaluate local climate change impacts [40]. The climatic conditions, orography, and lithology of an area influence the effects of climate change, and for this reason each territory could be subjected to different effects and must be studied specifically.

2. Case Study Area

The case study area is the Valtellina valley, in the Rhaetian Alps of Italy, in practice overlapping the Adda river watershed (Figure 1, near the outlet at Como Lake, 5118 km²).

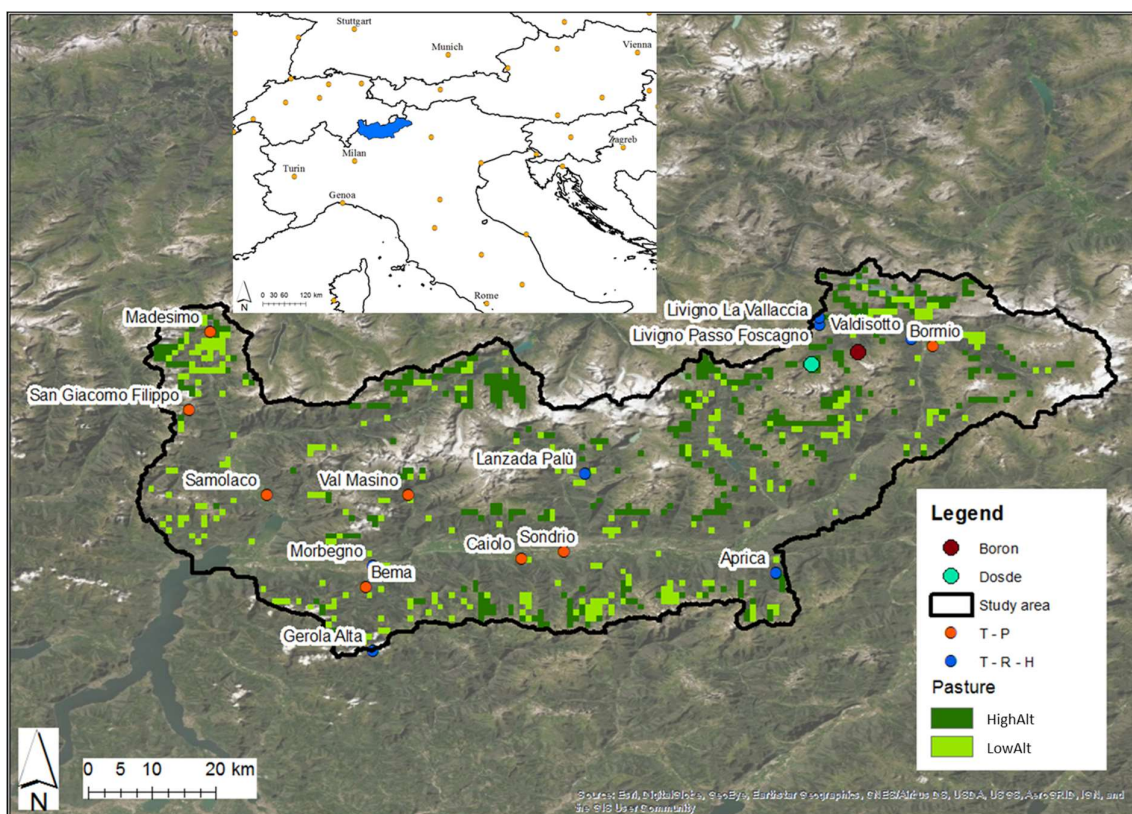


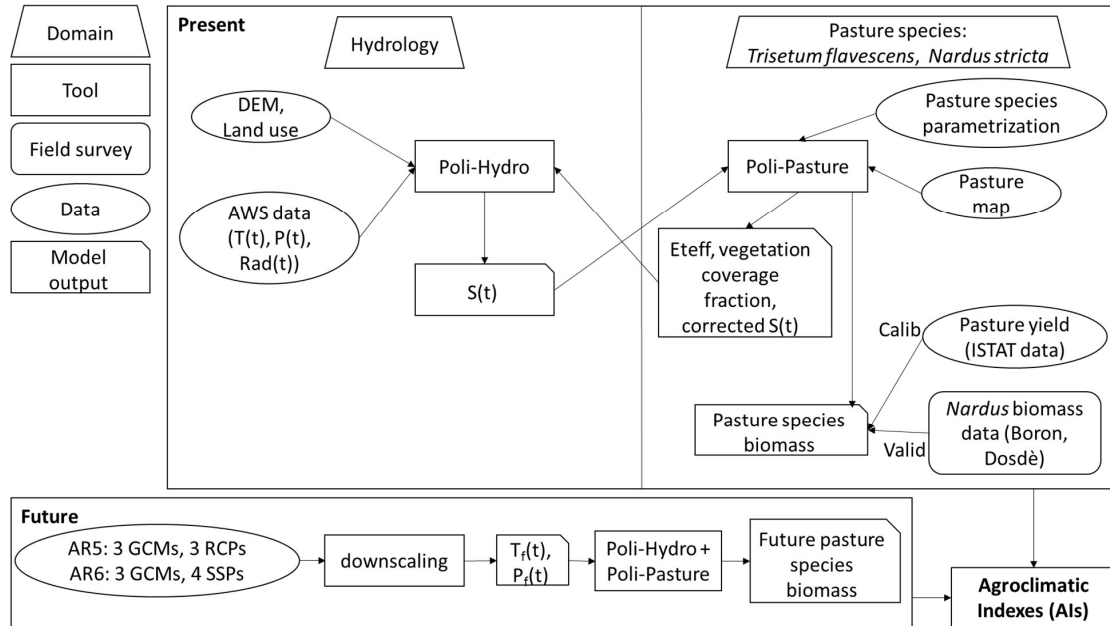
Figure 1. Map of the study area: location of two experimental sites of Boron (dark red) and Dosde (light blue) and of automatic weather stations AWS (orange stations (T-P) provide temperature and total precipitation, blue stations (T-R-H) provide temperature, rain (liquid precipitation) and snow depth). The pasture area, identified from a Corine Land Cover map (CLC, 2012), is reported as per altitude belts HighAlt (>2000 m asl) and LowAlt (<2000 m asl). In the white map, the geographic location of Valtellina and Valchiavenna within the Alpine belt is shown.

The study area covers a large altitude range, from 225 to 3610 m asl. Valtellina has a temperate climate, with no dry seasons and a warm summer, classified as *Cfb* in the Köppen–Geiger climate classification [43]. Yearly precipitation P in the area averages 1400 mm y^{-1} (1422 mm y^{-1} below 2000 m asl, 1383 mm y^{-1} above 2000 m asl). Precipitation has no large lapse rate in elevation. Usually, however, P is more abundant in the western part of the valley (nearby Como Lake, e.g., Morbegno, 1137 mm y^{-1}) than in the eastern part (e.g., Livigno–Foscagno, 670 mm y^{-1} , see also [44]). The mean annual temperature, T , is $+1.5 \text{ }^{\circ}\text{C}$ above 2000 m asl and $+5.0 \text{ }^{\circ}\text{C}$ below 2000 m asl. It reaches $0 \text{ }^{\circ}\text{C}$ at Livigno La Vallaccia (2660 m asl) and $+14 \text{ }^{\circ}\text{C}$ in Morbegno (230 m asl). The summer temperature peaks in July at around $+23 \text{ }^{\circ}\text{C}$ in Morbegno and $+8 \text{ }^{\circ}\text{C}$ in Livigno. The winter temperature reaches $-8 \text{ }^{\circ}\text{C}$ and $+3 \text{ }^{\circ}\text{C}$, respectively.

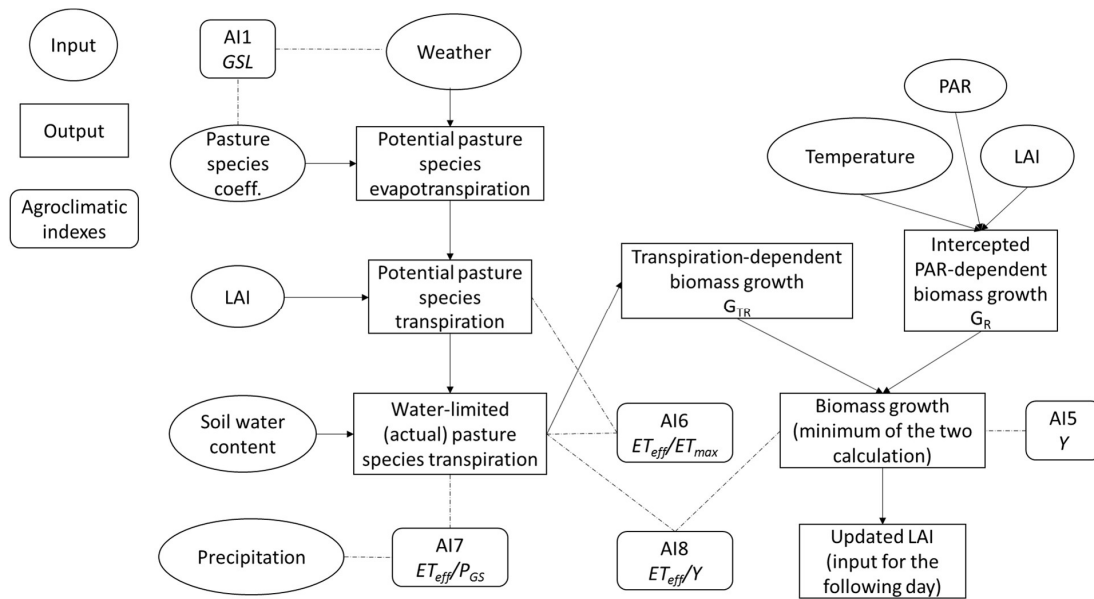
Pasture and grassland cover an area of 522 km^2 within the basin (Figure 1). A large spatial variability of pasture productivity is present because of differences in temperature (i.e., altitude), soil fertility, precipitation, and soil moisture conditions [45]. Usually, productivity (tons of dry product per hectare per year) may range within $0.5\text{--}6.5 \text{ t}_d \text{ ha}^{-1} \text{ y}^{-1}$. In Valtellina, bovines, ovines, and caprines graze on grasslands and pastures. In particular, during the spring and early summer, animals graze at low altitudes, and then during the summer grazing is moved upward to the pasture lands. The grazing may be free or controlled. In the first case, animals, especially bovines, can move for preferred grass. The second case applies principally to ovines/caprines and animals gathered in defined areas, where grass is at the optimal growth stage. Animals optimize their consumption, and it is possible to control the growth of good pasture species [46,47].

3. Data and Methods

In Figure 2, two flow charts of the methodology used here are reported, while in Appendix A, a summary of the two models used here is given.



(a)



(b)

Figure 2. (a) Flow chart of the methodology: the setting is presented on the top left. Poli-Hydro (hydrology) and Poli-Pasture (pasture growth) components and interconnections are reported in the frame on the top, named “present”. Generation of future projections is presented in the frame below, called “future”. T , P , and Rad are meteorological data: temperature, precipitation, and radiation, respectively. $S(t)$ is the soil water content, and ET_{eff} is actual evapotranspiration. (b) Detailed flow chart of Poli-Pasture model: depicting operation at a generic time step t . Inputs are data, Poli-Hydro-simulated variables at time step t , and Poli-Pasture-simulated variables at the previous time step. Outputs are used for the agroclimatic indices calculation and as input to Poli-Hydro and Poli-Pasture at the following time step.

In practice, the hydrological model *Poli-Hydro* is coupled with a pasture module *Poli-Pasture* to be able to simulate pasture dynamics starting from some outputs of the hydrological model: e.g., the spatialized daily temperature, the on-ground radiation, and the simulated availability of water for plant growth.

The principal purposes of the work are: (i) to simulate distributed pasture productivity in a watershed to have results on a large area and to identify differences in zones; (ii) to study the timing of plant growth, using both a simulation with both fixed growing season and variable growing season; (iii) to understand if synthetic indices could be useful to identify causes of growth limitation.

After the calibration of the model with the two growing season schemes, the agroclimatic indices were defined. To conclude, future projections were performed using scenarios of the IPCC AR5 and AR6. It was possible to analyze different results of the two assessment reports, the overall impact of climate change on pasture dynamic and growth, and the efficacy of the chosen agroclimatic indices.

3.1. Hydrological and Pasture Model

The *Poli-Hydro* model is essentially a spatially semi-distributed (i.e., with distributed budget, simplified cell-by-cell flow routing, independent cells, and lateral flows neglected) model, which applies mass conservation (continuity) equations to water content in the soil between two consequent time steps. The model (see [48,49]) is suitable for assessment of water budget and cryospheric dynamics in high-altitude areas (e.g., [50]). The study area was partitioned in a grid with cells of $1 \times 1 \text{ km}^2$, and for each time step (here, 1 day) the required variables were evaluated. The *Poli-Pasture* module [24,33,51] iteratively receives from *Poli-Hydro* the daily value of soil water content, to evaluate the growth of vegetal/agricultural species for the same time steps, and cells. The *Poli-Pasture* module returns to *Poli-Hydro* a daily value of leaf area index (LAI), used to assess correct daily evapotranspiration, fraction of soil with vegetal coverage, and soil water content (used for the vegetation growth).

Potential evapotranspiration ET_{max} was calculated using Priestley–Taylor’s formula in pasture areas and Hargreaves’ formula in non-pasture areas.

Then, the model estimated actual (soil moisture-driven) evapotranspiration ET_{eff} . Comparing the two values (ET_{max} and ET_{eff}), it was possible to highlight water stress resulting from low precipitation and/or high temperature. Evapotranspiration, in the presence of vegetation, depends upon the LAI, which was calculated daily, based upon the daily vegetation growth, its vegetative stage, and soil water content [52].

The growth stages of the pasture species were assessed based upon accumulation of thermal time stages (degree-days DD [$^{\circ}\text{C}$]). During the growing season (GS) [30], a new stage is reached when the accumulated thermal time reaches a proper threshold. If the daily temperature is below a base temperature T_{base} , no thermal time is accumulated, and if the daily temperature is larger than a cutoff temperature T_{cutoff} , the growth is limited. Model tuning was attained by varying degree-day thresholds for each growth stage (beginning of growth, flowering, maturity, end of growth). The *Poli-Pasture* module estimates daily production of biomass for each species, i.e., the minimum value between (i) water-dependent growth G_{TR} and (ii) solar radiation growth G_R .

For the simulation, proper dates for the growing season start/end needed to be chosen. GS started on April 1st in LowAlt and on April 30th in HighAlt, while the end of GS was taken on September 30th in both zones [53]. At low altitude, the *Trisetum flavescens* is harvested just before the maturity, while *Nardus stricta* at high altitudes is fed to animals just after the flowering, as reported in literature (e.g., [45,54]). After cut/feeding, growth starts again, and the cycle is repeated until the end of the GS. The total annual production in a cell is calculated as the sum of peak biomass in each growth cycle.

Then, the same simulation was carried out considering a variable growing season. GS would start when the mean temperature would be higher than T_{base} (for each species) for 10 consecutive days, and it would stop when T would be lower than the mean temperature

of September 30th (during the period 2006–2019) (i.e., the expected end of the GS) for 10 consecutive days. This may account for yearly potential variations of the growing season length, in response to specific climate conditions. In doing so, it was possible to (i) improve the results of simulation, and (ii) evaluate the impact of the future modified climate upon species' growing season length, therefore and productivity.

3.2. Weather Data

The *Poli-Hydro* model is driven by meteorological data, namely temperature, (total) precipitation (then properly split into solid/liquid), and radiation, and it gives as output estimates the soil moisture, evapotranspiration, and (total, overland plus sub-superficial) runoff. It was run here at the daily scale, suitable for pasture simulation (e.g., [24]).

Weather data are made available by ARPA Lombardia (the regional agency for environmental protection, www.arpalombardia.it, accessed on 3 November 2022). For this study, 15 ARPA stations were used (see Figure 1 and Table 1). During 2003–2019, each station measured daily data of (air) temperature T . A total of 8 stations provide total precipitation P (heated rain gages, including solid precipitation), while 7 others separately provide rainfall R and snow depth H (the latter via sonic snow gauging), always at the daily scale. When snow depth H data are available, one can assess daily new snow depth H_n and then convert it into new snow water equivalent (SWE_n). Here we took a mean snow density of 115 kg/m^3 , valid in the area [55,56].

Table 1. Meteorological stations considered for the model: elevation, position, and measured variables. T is temperature, P is total precipitation (heated rain gauge), R is (liquid) rainfall, H is snow depth. The location of the stations is visible in Figure 1.

Station	Altitude [m asl]	Latitude [°]	Longitude [°]	Variables
Aprica	1950	46.13	10.15	T, R, H
Bema	930	46.11	9.57	T, P
Bormio	1172	46.45	10.37	T, P
Caiolo	274	46.15	9.79	T, P
Gerola Alta	2178	46.02	9.58	T, R, H
Lanzada Palù	988	46.27	9.88	T, R, H
Livigno La Vallaccia	2660	46.48	10.21	T, R, H
Livigno Passo Foscagno	2320	46.49	10.21	T, R, H
Madesimo	1915	46.47	9.35	T, P
Morbegno	230	46.14	9.58	T, R, H
Samolaco	206	46.24	9.43	T, P
San Giacomo Filippo	2057	46.36	9.32	T, P
Sondrio	290	46.16	9.85	T, P
Val Masino	934	46.24	9.63	T, P
Valdisotto	1537	46.46	10.34	T, R, H

Data were collected for the present period (2003–2019), in practice the overall simulation period of the model. During the present period, a control run period CR (2006–2017) was identified for the calibration of the model and as a reference for the future projections and the downscaling process (Section 3.5), and a validation period in the years 2003, 2004, and 2019.

The *Poli-Hydro* model needs distributed daily meteorological data, i.e., a value of temperature and precipitation for each time step and each cell. Thus, AWS daily data

were spatialized considering Thiessen polygons around each AWS and applying a monthly altitudinal gradient (for T and P) calculated from the AWS data and their elevation.

Solar radiation was calculated on a distributed basis (i.e., in every cell of the model), based upon theoretical extraterrestrial radiation, topographically corrected for shading ([57]).

3.3. Land Cover and Soil Properties

A land cover map was used to estimate the maximum soil retention potential S_{Max} (necessary to pursue *Poli-Hydro* simulation) within the study area, based upon the SCS-CN method [58], and also to assess the area covered with vegetation (pastures in particular) and with rocks and ice, etc. This map was made available under the umbrella of the Corine Land Cover (CLC, 2012) experiment of the European Copernicus Programme. The *Poli-Hydro* model requires as inputs the hydraulic properties of soil, namely wilting point θ_w , field capacity θ_l , saturation θ_s , hydraulic conductivity K , in turn depending on soil texture [59] and the depth of the active soil layer, considered here constant for the entire area, based on the average properties of the Valtellina territory. Soil properties used for hydrological modeling were also made available in fulfilment of other studies of the area of Valtellina [48,57,60].

3.4. Pasture Productivity

The *Poli-Pasture* module runs jointly with the *Poli-Hydro* model to calculate pasture species productivity. *Poli-Pasture* was tuned here using pasture yield statistics, as reported by ISTAT (i.e., the National Institute of Statistics), aggregated for each province of Italy. Valtellina and Valchiavenna (included in the study area) cover the whole territory of Sondrio province, and accordingly the total production simulated by the model in the considered area is comparable to the data given by ISTAT for that province.

Pasture lands in Valtellina are substantially divided into two areas, namely high-altitude pastures, above 2000 m asl (henceforth pasture zone HighAlt), and grasslands at low altitude, below 2000 m asl (pasture zone LowAlt).

In fulfilment of the MOUPA project, data of pasture (*Nardus stricta*) biomass and relative species abundance were collected in the Dosdè area (Figure 1) during summer 2019 (2 different sites, Dosdè 1, 2100 m asl, and Dosdè 2, 2500 m asl, Confalonieri R., personal communication, 2020). Based upon the available literature, and upon results from collected samples under the umbrella of the MOUPA project, within the HighAlt/LowAlt zones we could identify some more abundant species. Above 2000 m asl, the most abundant species retrieved was *Nardus stricta* (henceforth *Nar.*), while below 2000 m asl *Trisetum flavescens* (henceforth *Tris.*) was predominant [53,54]. In particular, in the first considered site of Dosdè, *Nardus stricta* is the second most abundant with a presence of 10.25% in July and 34.47% at the end of August; in the second site, it was the most abundant species with a percentage of 84.45% in July and 77.44% in August. Therefore, these species were preliminarily considered as representative of the pasture vegetation in the area [45,61] and their growth was simulated. More realistic pasture growth simulation may require modeling of multispecies growth and their intraspecies and interspecies competition [25,62]. However, for our purpose of preliminarily assessing potential impacts of climate upon pasture productivity in this area, the hypothesis of monoculture pastures may be seen as representative of bulk pasture behavior (e.g., [24]). For the simulation, specific parameters of growth were collected for both species [52,63–65]. In Table 2, the parameters used for simulation with the *Poli-Pasture* model are reported for both species. The values of these parameters were mostly collected from literature (see e.g., [24,26,33,66–68]), and some were tuned with manual calibration. The reported values of DD factors were cumulated since the beginning of the GS.

Table 2. Poli-Pasture module parameters: their value for *Nardus stricta* and *Trisetum flavescens*. Parameters in **bold** calibrated against yield data from ISTAT. Other parameters taken based upon literature. a: [68], b: [67], c: [33], d: [24], e: [26]. *DD* factors are taken since growth season GS start.

Variable	Symbol	Unit	<i>Nardus stricta</i>	<i>Trisetum flavescens</i>	Reference
Mean daily temperature optimal growth	T_{opt}	°C	12.00	17.00	a, b, d, e
Biomass-transpiration coefficient	BTR	kPa kg m ⁻³	5.00	6.50	d, e
Conversion light-biomass parameter	$LtBC$	g MJ ⁻¹	1.30	2.50	d, e
Real/potential transpiration, end of leaf growth	AT/PT	-	0.50	0.50	c
Max daily water absorption	U_{max}	kg m ⁻² day ⁻¹	13.00	15.00	d, e
Hydr. leaf potential, onset stomatal closure	psi_{sc}	J kg ⁻¹	-2500.00	-2800.00	d, e
Hydraulic potential, leaf wilting	psi_{w}	J kg ⁻¹	-2300.00	-2400.00	d, e
Morphology					
Max root depth	Rd_{max}	M	0.30	0.80	d, e
Maximum radical density	D_{max}	cm ⁻²	3.00	4.00	c
Initial leaf area index	LAI_0		0.00	0.00	-
Specific leaf area	SLA	m ² kg ⁻¹	25.00	35.00	d, e
Partition stem/leaf	Ls	m ² kg ⁻¹	2.00	3.00	d
Degree-day leaf	DD_{leaf}		500.00	600.00	d
Extinction coefficient of solar radiation	k_{alfa}	-	0.40	0.50	d, e
Cultural evapotranspiration coefficient	Kc_0	-	0.75	0.85	d, e
Phenology					
Degree-day emergency	DD_{emerg}	°C d	50.00	50.00	a, d
Degree-day flowering	$DD_{flowering}$	°C d	400.00	400.00	a, d
Degree-day maturity	$DD_{maturity}$	°C d	800.00	800.00	d
Degree-day for Rd_{max}	$DDrd_{max}$	°C d	300.00	300.00	-
Base temperature	T_{base}	°C	5.00	8.00	a, b, d
Cutoff temperature	T_{cutoff}	°C	18.00	21.00	a, b, d
Harvest					
Harvest Index	HI	-	0.70	0.70	e
Degree-day harvest	DD_{har}	°C d	500.00	650.00	-

ISTAT reported estimates of total annual production Y_y [t] (2006–2017) in the Sondrio province, but pasture area therein varied during the years. Indeed, the area used for grasslands and pastures decreased during the study period, according to ISTAT information. Such changes are not justified in the ISTAT report and might have been influenced by social and economic factors, not amenable to modeling here, such as land abandonment for personal reasons, generational changes, or lack of public funding. Accordingly, specific (to area) production Y was then used for calibration purposes. Model tuning was pursued according to an objective score, namely the percentage mean error *Bias*. An acceptable calibration would be attained if $|Bias| < 10\%$. Given the small amount of data for tuning (i.e., 14 yearly values of Y), other more sophisticated adaptation statistics (root-mean-square error RMSE and root-mean-squared percentage error RMSE%) were not used for tuning, but were, however, calculated and are reported further on.

It was not possible here to verify growth timing and spatial distribution of biomass in the area, given the lack of in situ data or spatially distributed information. However, the growth patterns of the two species were compared against those found in other studies about pasture [24,45], and Y was compared against literature values. At high altitudes in the Alps, productivity of pastures was estimated to be near to 3–4 t ha⁻¹, while below 1000 m asl higher values could be found, around 8 t ha⁻¹ [45,54]. Here, it was also possible to gather an in situ estimation of specific annual production (of *Nardus stricta*) at high altitudes in the area of Valtellina valley. This came from the available literature, specifically in Alpe Boron (Figure 1), during 2003 and 2004 [69], and from production data collected in the Dosedè area in fulfilment of the MOUPA project, and could be used here for the benchmark.

3.5. Climate Projections and Future Simulations

Once properly tuned, *Poli-Hydro* and *Poli-Pasture* were used to project pasture production during 2020–2100 (i.e., after the end of the present period 2003–2019). After a preliminary screening, 21 scenarios were generated, combining different GCMs and RCPs/SSPs, to analyze the response of our pasture species growth to different pathways of the climatic drivers. Particularly, the selected GCMs are able to acceptably describe the climate of Northern Italy, especially in terms of the seasonality of precipitation [18,29,70]. However, local downscaling is required to properly mimic local weather statistics at specific points [17].

The simulation was conducted under a variable GS, under three representative concentration pathways (RCPs) of the Fifth Assessment Report of IPCC, RCP 2.6, RCP 4.5, RCP 8.5. Three atmospheric and ocean general circulation models (AOGCMs) were used, downscaled to the area of study, from the Coupled Model Intercomparison Project, release 5 [71], namely, ECHAM6.0 (European Centre Hamburg Model, version 6, [72]), CCSM4 (Community Climate System Model, version 4, [73]), and EC-Earth (European Consortium Earth system model, version 2.3, [74]). Simulations were also carried out using projections under the umbrella of the Sixth Assessment Report AR6 of IPCC, namely for SSP 2.6, SSP 4.5, SSP 7.0, and SSP 8.5. Three GCMs were chosen from the CMIP6 [75], EC-Earth3 (European Consortium Earth system model, [76]), ECHAM6.3 (Max-Planck-Institute für Meteorologie, [77]), and CESM2 (Community Earth System Model, [78]).

In general, GCMs display a variable spatial resolution, in the order of $100 \times 100 \text{ km}^2$ or so, and downscaling needs to be pursued to gather daily series of temperature and precipitation at the spatial resolution of $1 \times 1 \text{ km}^2$ for the *Poli-Hydro* model. For precipitation, a stochastic space random cascade model (SSRC, [70]) was used. This method provides downscaled series that are statistically consistent (i.e., displaying the same properties of mean, variance, and intermittence for rainfall) with the locally observed data, but conserve the trends as provided by the GCM models. Temperature series were downscaled using a ΔT approach [17], in which an average monthly difference of temperature between the GCM series and the observed series calculated in the control run CR period (2006–2017) was applied to the projected GCM series, largely depending upon local altitude. By downscaling each GCM and scenario separately, spatially distributed, daily projected precipitation and temperature scenarios were obtained and used to feed the *Poli-Hydro + Poli-Pasture* model. Model parameters are held constant in the future in lack of any other hypothesis, and the area of pasture is the same, although chances for changes may occur.

It was decided to simulate both AR5 and AR6 because of the differences in their projections. For example, AR6 shows more pronounced increases of temperature with respect to AR5 for all GCMs and all scenarios. Considering precipitation, GCMs for the AR6 seem to be more unanimous in the projections [79]. Generally, GCMs for the AR5 project a large increase or large decrease in precipitation, while for the AR6 all project a contained reduction.

3.6. Agroclimatic Indices

We selected some agroclimatic indices (henceforth AIs), usable as indicators of climate change effects on pasture species productivity. We chose some indices from the available literature [22,31–39], including indicators of (i) climate, (ii) pasture productivity, and (iii) water availability and use. The chosen indices are reported in Table 3. These 8 AIs were selected because they concern different factors (average temperature of the spring and summer seasons, extreme temperatures, intermittence and quantity of precipitation, relation between water demand and availability through evapotranspiration assessment, etc.), giving a broad overview of the dynamics of our pasture species.

Table 3. Selected agroclimatic indices for the project: indices AI1–AI4 calculated from climate data/projections. Indices AI5–AI8 calculated using *Poli-Pasture* model. a: [31], b: [39], c: [33], d: [34], e: [35], f: [36], g: [37], h: [38].

AI	Variable	Symbol	Unit	Reference
AI1	Growing season length	GSL	d	b, f, g
AI2	Heat waves frequency (number of consecutive days with $T > T_{cutoff}$)	f_{HW}	d	b, f, g, h
AI3	Number of days in GS with precipitation > 10 mm	d_{10}	d	f, g
AI4	Total precipitation in growing season	P_{GS}	mm	g
AI5	Annual species productivity	Y	t	a, c, e
AI6	ET efficiency (in GS)	$ET_{eff}/ET_{max,GS}$	mm/mm	-
AI7	ET relative (in GS)	ET_{eff}/P_{GS}	mm/mm	-
AI8	Specific (green) water footprint (in GS)	ET_{eff}/Y	mm/t	c, d

Index AI1 provides the length of the growing season, and clearly, it was calculated only under the variable GS mode. Index AI2, or frequency of heat waves, and AI3, days with heavy precipitation during the growing season GS, represent the variability of stress factors for the species. Index AI4 of total precipitation indicates abundance/lack of rainfall for vegetation growth. Index AI5 provides an indication of (total) species biomass in the area. AI6, namely the ratio of yearly actual-to-potential evapotranspiration in the GS season, assesses the efficiency of species water use, in turn depending upon water availability and distribution in time (e.g., [34]). If this ratio is close to 1, plants use most of the available water, with large evapotranspiration efficiency. In AI7, relative ET is an indication of the necessary evapotranspiration with respect to the available water (precipitation, i.e., rainfall) in the GS period. This depends upon temperature (driving $ET_{max,GS}$) and available precipitation P . Specific water footprint AI8 is an indication of how much water (ET_{eff}) is needed to be used for the production of a ton of biomass (e.g., [80]).

AI values were calculated under present and future conditions for each RCP/GCM under AR5/AR6. The indices AI1–AI4 could be assessed using only climate data. Accordingly, climate data from the available stations were used for calculation under present conditions, while climate projections were used for future conditions. The indices AI5–AI8 explicitly depict the pasture species performance, and they were calculated using *Poli-Pasture* model's outputs under present and projected climate.

4. Results

4.1. Pasture Species Productivity in the Present Period (2003–2019)

4.1.1. Calibration of the Model Using ISTAT Data in the CR Period (2006–2017)

Poli-Pasture calibration was pursued by iteratively changing the tuning parameters (Table 2) to mimic the observed values of specific annual production Y from ISTAT (2006–2017). Clearly, the robustness of the parameters' tuning is of interest, and a sensitivity analysis within the parameters' viable space could be pursued [81]. However, here we were more interested in choosing the parameters' values that were most suitable to properly simulate the plants' dynamics. This was reasonable, given also that we possessed some data, useful to reasonably constrain the uncertainty in model tuning. A preliminary analysis here, and in other former studies, demonstrated that DD factors are in practice most affecting the performance of the model; thus, proper tuning is required.

The calculated percentage error, or $Bias_{\%}$, for the simulation with fixed GS was +10.82%, considering the production per hectare Y (−4.90% considering the total production Y_y). In the simulation with variable GS, $Bias_{\%}$ was −0.18% for Y (−9.93% for Y_y). Such a difference between Y , and Y_y may depend on changes in the pasture areas during the study period, as reported above. Goodness-of-fit statistics for Y for *Poli-Pasture*—i.e., $Bias_{\%}$, random mean square error, absolute $RMSE$, and percentage $RMSE_{\%}$ —are reported in Table 4. Determination coefficient R^2 was not calculated. Due to (possibly unlikely) constant values

of Y , as declared by ISTAT during 2006–2007 and 2008–2012, the variance of the observed sample is very low, and accordingly, calculation of R^2 makes little sense.

Table 4. Goodness-of-fit parameters of Poli-Pasture simulation: calculated against ISTAT data 2006–2017.

	Y-Fixed GS	Y-Variable GS
<i>Bias</i> _% [%]	+10.82	−0.18
<i>RMSE</i> [t/ha]	1.66	1.73
<i>RMSE</i> _% [%]	37.81	39.48

In Figure 3, observed and simulated values of Y in the CR period are reported.

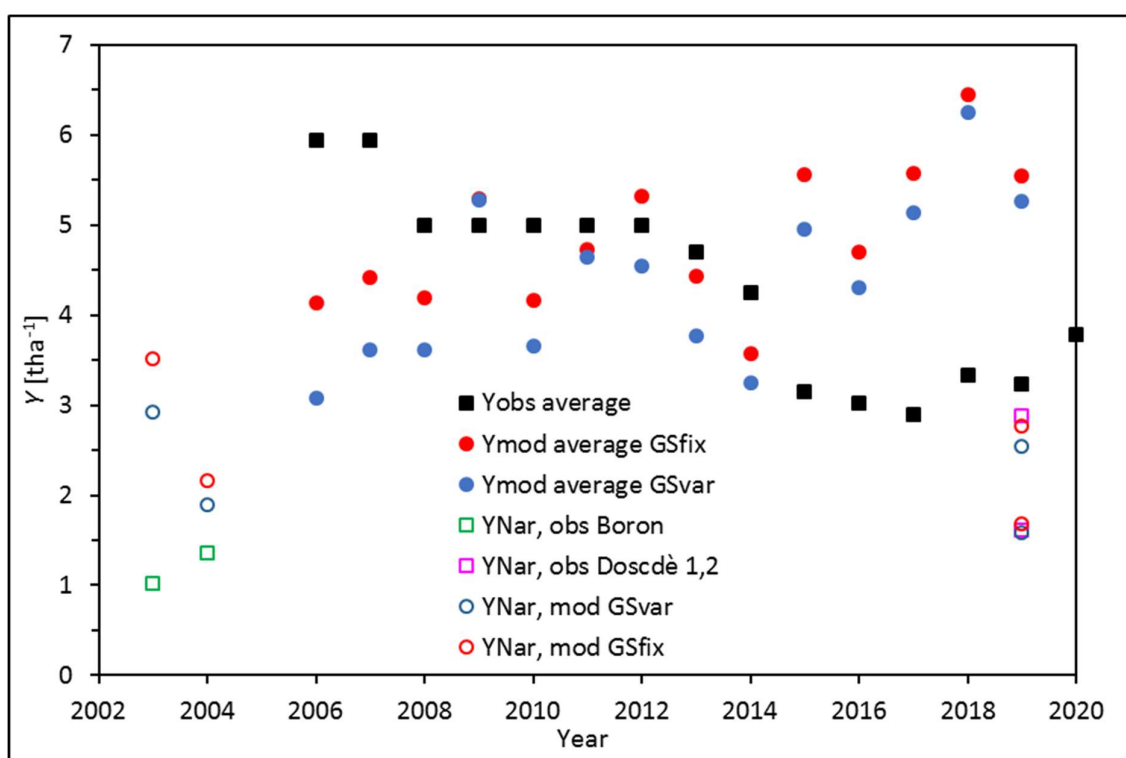


Figure 3. Simulated and observed annual pasture yields during 2003–2019: results of the simulations (red dots: fixed growing season; blue dots: variable growing season) are shown along with observed ISTAT data (full black squares) covering the whole Sondrio province. We report in situ data of biomass of *Nardus stricta* in Alpe Boron (2003–2004) (empty green squares) and Alpe Doscdè (2019, 2 sites) (empty pink squares), and the estimates from the simulation (empty red/blue circles) in the corresponding cells of the $1 \times 1 \text{ km}^2$ grid (see Figure 1 and Section 3.2).

4.1.2. Validation of the Model Using In Situ Data (2003, 2004, 2019)

For further model validation, in Figure 3 we reported in situ estimates of biomass of *Nardus stricta* in Alpe Boron (2003–2004) and Alpe Doscdè (2019, 2 sites), and the estimates from *Poli-Pasture* model, in the corresponding cells of our $1 \times 1 \text{ km}^2$ grid. Visibly, except for the year 2003 when some difference is spotted, in Boron the model simulates a specific productivity of 3.51 t/ha (fixed GS) and 2.92 t/ha (variable GS) instead of the observed value 1.03 t/ha. The *Poli-Hydro* model matches reasonably well with local (i.e., within a specific cell) estimates of pasture yield. In Table 5, the values of the difference in terms of specific productivity Y are reported for both the sites of Boron (for year 2004) and Doscdè (as average of the two sites). Such data were not used for model tuning, and accordingly, these results indicate an acceptable validation of the model.

Table 5. Differences in specific productivity between simulation and observation: in situ data were used for the validation of the model in Boron from the year 2003 and in Dosdè, for 2 sites, from the year 2019.

	Boron Fixed GS	Boron Variable GS	Dosdè Fixed GS	Dosdè Variable GS
ΔY [t/ha]	0.81	0.54	−0.02	−0.18

4.1.3. Uncertainties in Calibration Data

ISTAT data of pasture productivity give the yearly sum of the total production of three classes of pasture/grassland, namely permanent grasslands and pastures, poor pastures, and other pastures. These data are collected with an estimative methodology, based upon the evaluations of local experts, producers associations, questionnaires, and auxiliary data, etc. The estimates for 2006 and 2007 derive from a different campaign, with different guidelines for the statistics of plant-related products. Moreover, the class “poor pastures” appears only since 2013. Poor pastures have a lower specific production Y with respect to other classes of pasture, and they contribute to the reduction of specific production after 2013.

Because of these uncertainties related to ISTAT data, in addition to the comparison of specific productivity, we also compared the growth rate between the simulation results and the observation data. As reported in Figure 4, looking at the ISTAT data of productivity, only for permanent grassland and other pastures in the period 2006–2017 was there a growth rate of +0.11 t/ha/y, coherent with the result of our simulation (growth rate of +0.07 t/ha/y in the simulation with fixed GS, and of +0.10 t/ha/y in the simulation with variable GS). Moreover, as we can see in Figure 3, in 2015–2020 the overall (considering all three ISTAT classes of pastures) specific production also has a growing trend equal to +0.12 t/ha/y.

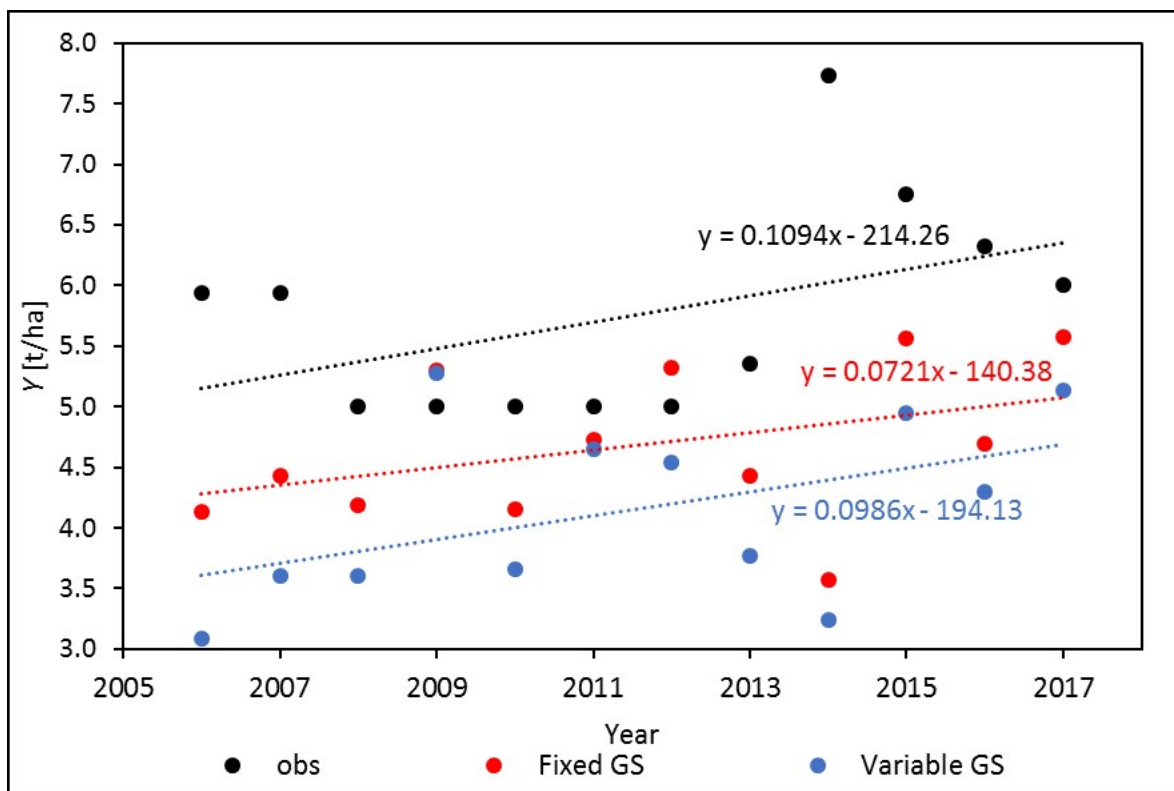


Figure 4. Trend in specific productivity Y : observed values of Y of permanent and other pastures are in black, while the result of simulations are reported in red and blue, considering fixed and variable GS, respectively.

Given the complexity of the vegetation modeling exercise and the potential for some uncertainty in ISTAT estimates of both yield and of pasture-covered areas, *Poli-Pasture* estimates seem acceptable, at least on average. Furthermore, given the fact that we are interested in assessing relative changes in the yield potential of our pasture species under climate change, the model's estimates can be taken here as useful for the purpose.

The yield of pasture species Y and Y_y could also be evaluated as per altitude belts, ranging from 200 to 2600 m asl. The study area was divided into eight belts of 300 m of altitude, each one displaying a different area. In Figure 5, the distribution of Y_y , and Y as per altitude belts is reported for the year 2017; however, the altitude pattern is very similar for every year during the present period.

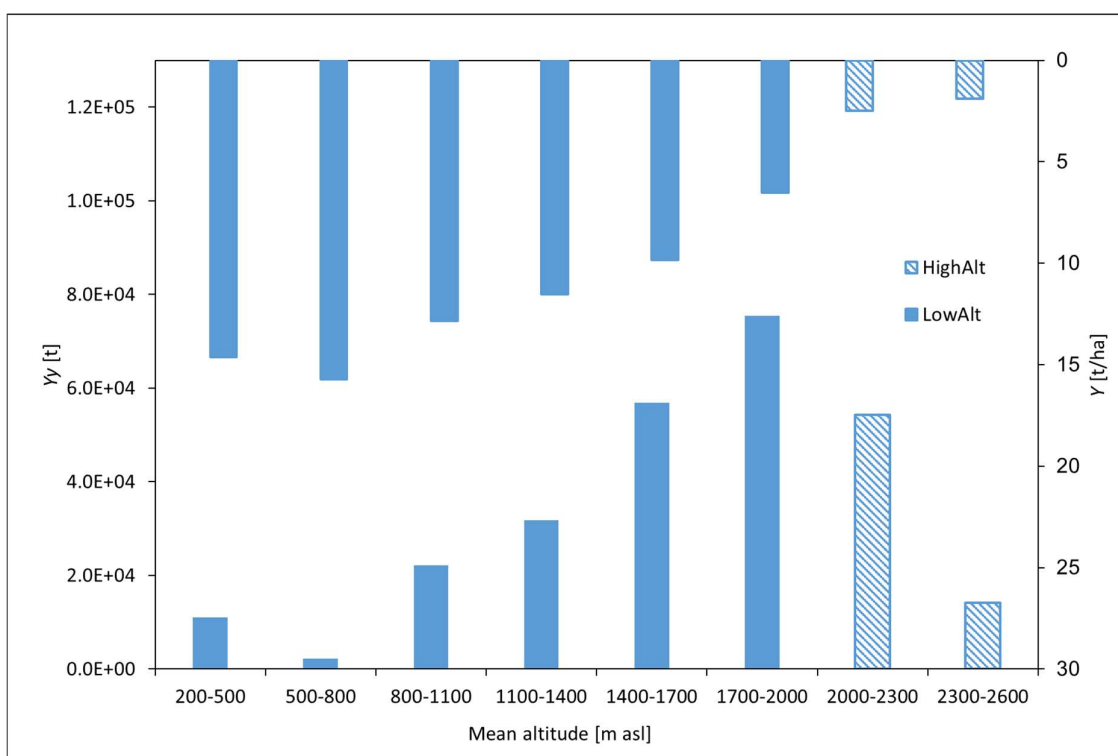


Figure 5. Pasture productivity: simulation of total production of pasture species Y_y (left ordinate axis) and specific production Y (right ordinate axis, upside down) as per altitude belts for year 2017, considering variable GS. Zone HighAlt and zone LowAlt.

A largest yield Y can be seen between 1700 m asl and 2000 m asl (with *Tris.*) and between 2000 and 2300 for *Nar.*, where, however, the specific production Y is quite low (but clearly a large area for pasture cropping is available).

4.2. Future Pasture Species Productivity

Given the outputs of the model tuning exercise, we decided to simulate the future growth of our pasture species under a variable GS mode, especially to be able to highlight changes in the duration of the suitable season for species growth. Generally, an increase in productivity is expected. This is principally due to an increase in T . Indeed, temperature increases potential evapotranspiration ET_{max} . If enough water is available, actual evapotranspiration ET_{off} also increases, thus increasing ET -dependent biomass growth (Equation (A8)). Increased temperatures lead to a quicker achievement of saturation of the degree-day, with consequently faster maturity and possibly more growth cycles during GS. Looking at AR5, for all models, under RCP 2.6 the differences between the period 2041–2050 and the period 2091–2100 are small, but for RCP 8.5, ΔY is significantly larger for 2091–2100 than for 2041–2050. In general, variations during 2091–2100 are larger for AR6 than for AR5.

Similar results were found when considering the two main altitude zones but with variations in HighAlt larger than in LowAlt. The range of variation ΔY (mean, min, max) among all models and RCPs as per altitude belts during 2041–2050 and 2091–2100 is reported (Figure 6). In HighAlt (>2000 m asl), the percentage variation $\Delta Y\%$ is larger than in LowAlt. However, considering the absolute values of Y , future productivity would still be smaller in HighAlt (*Nardus stricta*) than in LowAlt (*Trisetum flavescens*). The main difference between AR5 and AR6 is that, according to the latter, during 2041–2050 and 2091–2100 similar changes ΔY would be seen (Figure 6b), differently from AR5 (Figure 6a). Above 1700 m asl or so, AR6 projects a larger variation for 2041–2050 and less for 2091–2100 than AR5. Moreover, in some belts (200–500 m asl and 800–1100 m asl) under AR5, productivity would slightly reduce until -18% on average (Figure 6a, 3rd belt, 2041–2050) within a range reaching -31% , and the reduction would be larger in 2041–2050 than in 2091–2100. In AR6, there would be a reduction for the same belts, slightly larger in 2091–2100 than in 2041–2050, and smaller than in AR5, namely reaching until -27.40% (Figure 6b, 3rd belt, 2091–2100). On average, however, reduction would only occur in the first belt (-10%).

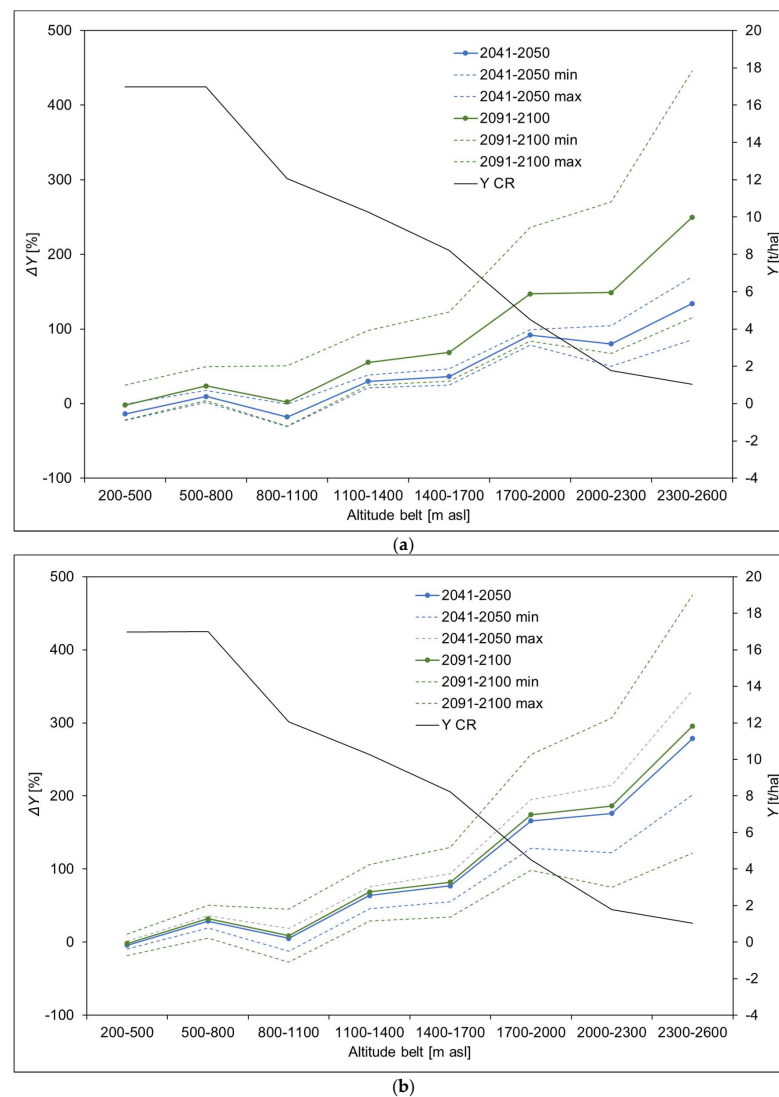


Figure 6. Percentage variation of specific production: percentage variation (mean, max, min, left ordinates axis) of specific production Y during 2041–2050 and 2091–2100, along with absolute values during the 2006–2017 (control run period, CR) for altitude belts ranging from 200–500 m asl to 2300–2600 m asl. (a) AR5, (b) AR6. Results above refer, respectively, to *Trisetum flavescens* below 2000 m asl and to *Nardus stricta* above 2000 m asl.

4.3. Agroclimatic Indices

The values of AIs were assessed in every year of the CR period for *Trisetum flavescens* (<2000 m asl, LowAlt) and *Nardus stricta* (>2000 m asl, HighAlt). Then, the AIs were calculated for the future projections during 2041–2050 and 2091–2100, for each model and RCP, with variable GS mode. All AIs are reported in Figure 7. The figure presents the average values (among all GCMs) of the indices for each scenario, also benchmarked against values in the control run period CR (2006–2017) for *Nardus stricta* (HighAlt, >2000 m asl) and *Trisetum flavescens* (LowAlt, <2000 m asl), at the middle (2041–2050) and at the end (2091–2100) of the 21st century.

Generally, a potential extension of GS (i.e., a longer growing season, AI1, Figure 7a) during 2041–2050, and 2091–2100 is seen with few exceptions under AR5. Moreover, AR6 projections show a larger extension of GS with respect to AR5 projections. Longer GSL is due both to an earlier onset of GS and to a later end of GS due to higher temperatures in the spring and fall. This clearly contributes to the increase in yield Y (AI5, Figure 7e) because of (i) the longer time for growth and (ii) the chances for more growth cycles (harvest/feed). However, a significant increase in temperature, with more frequent heat waves (AI2, Figure 7b), may be a limitation for plants' growth and may justify the potential decrease in Y in Figure 6 (low altitude belts–LowAlt). Comparing projections of AI3 (days with $P > 10$ mm, Figure 7c) and AI4 (total precipitation during GS, Figure 7d), mostly a reduction of precipitation brings a reduction of intense precipitation days, and vice versa, with some exceptions, both during 2041–2050 and 2091–2100.

Index AI6, ET efficiency, or the ratio ET_{eff}/ET_{max} (Figure 7f) increases in 2041–2050 and 2091–2100 in both HighAlt and LowAlt, in spite of mostly decreasing precipitation. Indeed, in our simulations, ET_{eff} increases more than ET_{max} , possibly in response to (i) the longer growing season and (ii) the decreased incidence of extreme events (AI1, AI4) and subsequently more regular distribution of precipitation/soil moisture.

AI7, relative ET , or ET_{eff}/P_{GS} increases mostly (Figure 7g) in both HighAlt and LowAlt in 2041–2050 and 2091–2100. Under increased temperature, especially in the highest areas, more water from precipitation is used to fulfil ET requirements for plants' growth (resulting in increased yield, as reported in Figure 6).

Specific water footprint AI8, namely ET_{eff}/Y (Figure 7h), may increase or decrease depending on the combination of ET_{eff} , and Y dynamics.

Comparing AR5 and AR6 projections, relatively to AI6 no differences could be seen. However, a larger increase in ET efficiency is expected at high altitude with respect to low altitude (under 2000 m asl).

On the contrary, considering AI7 (relative efficiency), a larger increase is projected by AR6 scenarios, both above and under 2000 m asl (HighAlt and LowAlt). Considering there are no marked differences in the precipitation quantity during GS based on the selected AR, this means a larger increase in ET_{eff} for the AR6.

Considering the water footprint AI8, under the AR5 our GCMs usually project an increase for low altitude (LowAlt) and a decrease for high altitude (HighAlt) for most RCPs (with the exception of the ECHAM6.0 model). On the contrary for AR6 scenarios, the GCMs show a decrease in specific water footprint for both low and high altitude, generally with few exceptions.

In spite of the increase in ET_{eff} , highlighted by AI6 and AI7 in particular for the AR6, and in general for high-altitude areas (both AR5 and AR6), the large increase in productivity at high altitude and in particular for the AR6 explains the reduction of the specific WF (AI8). On the contrary, the decrease in productivity at low altitude explains the reduction of AI8 in LowAlt.

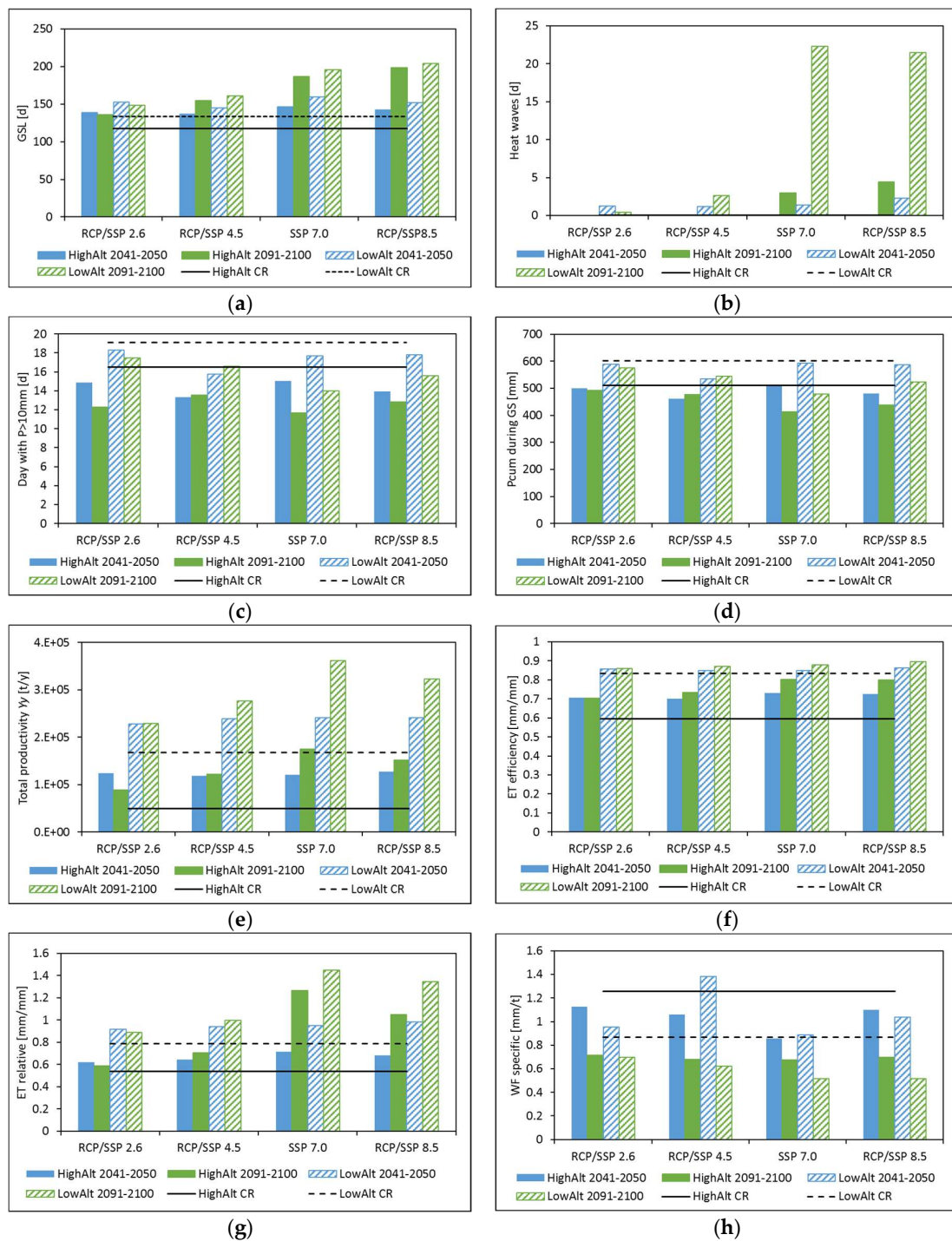


Figure 7. Future projections of agroclimatic indices (AIs) with respect to the control run (CR) period for two pasture species: (a) growth season length (GSL) (AI1), (b) heat waves frequency (AI2), (c) number of days with P larger than 10 mm (AI3), (d) cumulated P during GS (AI4), (e) productivity Υy (AI5), (f) evapotranspiration (ET) efficiency (AI6), (g) relative evapotranspiration (ET) (AI7), (h) specific water footprint (WF) (AI8). The reported values are the average with respect to the scenario (RCP/SSP 2.6; RCP/SSP 4.5; SSP 7.0; RCP/SSP 8.5) of all the GCMs. Values at the middle of the century (2041–2050) are reported in blue, while values at the end of the century (2091–2100) are in green. Values for *Nardus stricta* are reported in plain color (HighAlt, >2000 m asl), and values of *Trisetum flavescens* are reported with lines (LowAlt, <2000 m asl). Black lines refer to the present values (dotted for LowAlt and continuum for HighAlt).

5. Discussion

5.1. The Calibration of Poli-Hydro+Poli-Pasture Model

The use of the *Poli-Pasture* model, associated to the hydrological model *Poli-Hydro*, allowed here to link growth of our pasture species to the climate and water budget of the study area. The *Poli-Hydro* model is suitable for the simulation of high-altitude watershed hydrology, as in the case of Valtellina and Valchiavenna [29,48,57,60], thanks to the accurate formulation of snow melt and, in general, of water balance components. In [29], the authors report proper calibration of the hydrological model *Poli-Hydro* for the considered area. *Poli-Pasture* may therefore be used to simulate growth of high-altitude pasture species, differently from other models used for low grasslands [82–87]. Particularly, snow cover dynamics affect the growing season of pasture species and water availability, and simulation is thereby important in our target areas.

With proper hydrological simulation as a background, the modeled pasture species growth seems acceptably representative. The main issue with model tuning here was data availability, given that we could use only bulk pasture yield estimates at the large scale of the Sondrio province. These data carried information from areas of permanent/rich pasture and from other areas of transient/poor pasture with lower yield; however, they were not documented properly. The model performance was influenced by the lack (or paucity) of local data about pasture yield and management of pasture areas, and the large differences in altitude and climatic conditions within the study area (see e.g., [51]).

The results here provide errors smaller than 10% on average. Statistics of random error, i.e., $RMSE_{\%}$, near to 30% seem acceptable [33,88]. However, validation against some local, sparsely available *Nardus stricta* biomass estimates at high altitudes provides encouraging results. In addition, our findings are coherent with recent studies on pasture biomass ([24], focusing upon pastures in mountain areas of Sardinia; [26,69], focusing on Valtellina).

5.2. Projections of Potential Changes in Pasture Dynamic and Productivity

The results of our future projections seem well aligned with recent literature. GS would be longer (Figure 7a), and production of species would increase (Figure 4). Water-use efficiency would increase, as shown in Figure 7f. An upward shift is seen here in terms of a decrease in productivity at the lowest altitudes and of an increase at the highest altitudes (as described by e.g., [51] for crop species; [21,22]). Accordingly, one may investigate future potential for pasture colonization at the highest altitudes, as limited by area availability and topography (e.g., [51]).

Our results are further coherent with former studies about suitable areas for pasture growth. With the increasing summer temperature, pasture species may find optimal temperature conditions at higher elevations [23]. Indeed, one notices that below 1100 m asl (Figure 6), pastures may not find suitable conditions, and productivity may decrease. As reported in other cases (see e.g., [89,90]), *Trisetum flavescens* shows a potential decrease in presence and biomass in response to high temperatures in the summer, perhaps combined with a decrease in precipitation [90,91]. At higher elevations, above 2000 m asl, the large increase in productivity under climate change scenarios of the *Nardus stricta* may be explained by considering warmer temperature conditions and the properties of this species, which can adapt itself to drought conditions and needs less water than other pasture species [23,92].

Other studies demonstrated a potential increase in pasture productivity due to an increase in temperature and the subsequent reduction of snow cover duration. While in the CR period the growing season mostly overlaps with summer due to the optimal temperature range for growth, in the future potential anticipation of the GS, due to lack of snow cover, a sooner accumulation of thermal time, increasing densification and biomass of plants, anticipation of the peak of growth, and thereby an increase in productivity is seen [93,94].

From our calculated agroclimatic indices, (change in) annual pasture species productivity is driven by an increase in T during GS and less by P_{GS} , which would not be a limiting

factor in spite of the reduction of precipitation in some scenarios. As reported in other studies (e.g., [93,95,96]) grassland growth in Alpine catchments does not normally display water limitation, while low temperature at high altitudes may limit growth. In the results of this work, in future climate scenarios such limitation would be compensated by warming in all seasons. Water limitations may occur in some cases at the lowest altitudes, as driven by largely increased *ET* demand under temperature increase. Looking at Figure 7f,g, a small increase in *ET* efficiency and an increase in relative *ET* at low altitudes can be expected due to the reduction of precipitation. This explains the reduction of biomass for *Trisetum flavescens*, sensitive to drought periods.

An important novelty of this study is the use of updated IPCC AR6 scenarios and the comparison between AR5 and AR6.

In particular, we highlighted the larger increase in productivity and the more significant reduction of the specific water footprint for the AR6 scenarios.

5.3. Choice of Two Index Pasture Species

Clearly, in spite of the acceptable results here, improvements need to be pursued henceforth. The choice we made here of an index species (in each altitude zone) is clearly a simplified one, also taken in other studies [83,85–87]. Two of the most abundant species in the area were chosen. As reported, species abundance was verified using some data available in fulfilment of the project MOUPA (Confalonieri R., Movedi E., personal communication, 2020), namely samples taken during summer 2019 in the area of Dosdè catchment (Northwestern Valtellina/Valdidentro) above 2000 m asl. Thereby, *Nardus stricta* was the first or second most abundant species. Moreover, in the experimental site of Alpe Boron, *Nardus stricta* was the second most abundant species. Looking at other studies about the abundance of pasture species, *Nardus stricta* is often found in Alpine high-altitude pastures [97,98]. This is related to the ability of the species to adapt to different climate and soil conditions [23]. At low altitudes, under 2000 m asl, *Trisetum flavescens* is often present in alpine pastures and managed permanent grassland, where cuts are applied during the growing season [53,54,99,100]. For this reason, this species was used here as an indicator of low-altitude pastures. In dealing with a single species, simulation is faster, and it is possible to consider a large area, such as the Sondrio district here.

We maintained the spatial support for simulation (i.e., the pasture areas in the valley) unchanged in the future. In doing so, we could analyze the productivity of our target species on the whole territory, in contrast to other studies focused on single farm system [87,101], and identify better or worse areas for growth. Moreover, it was possible to evaluate the behavior of single pasture species and their reaction to the changing climate to consider its potential for livestock.

Clearly, changes of pasture composition in response to competition between species, and alterations in response to climate change, including shifting to higher/lower altitudes and abandonment of some areas, may happen in the future.

5.4. Limitations and Future Improvements of the Simulation

Interspecific competition between different species competing for nutrients, water, and light and with different periods of growth may modify the dynamics of pasture, also in response to climate variability (e.g., [25]). The development of a version of the *Poli-Pasture* model able to simulate competition between multiple species is ongoing; however, it requires a large amount of information of pasture composition and dynamics and further refinement. Notice further that the dynamics of pasture cover in space may also depend upon anthropic management, and accordingly, changes of the spatial extent of simulation in the future may need some hypothesis about land cover evolution. Such topics clearly indicate lines worthy of investigation henceforward.

The *Poli-Pasture* model does not explicitly account for the direct impact of extreme rainfall (storm) events, if not indirectly via increased runoff, and work in this direction may

be carried out. Further developments that could be discussed include assessment of the nutrient budget, given that the model assumes now full availability.

6. Conclusions

We analyzed the potential impacts of prospective climate change as projected under the IPCC AR5/AR6 scenarios upon two pasture and grassland species growth in the province of Sondrio in the central Italian Alps. We defined scores, or agroclimatic indices AIs, to objectively evaluate (i) climate suitability, (ii) pasture species productivity, and (iii) water use in the area.

An original contribution here concerns the use of a semi-distributed model for the simulation of high-altitude pasture areas over a large territory. Moreover, we projected future conditions considering new AR6 scenarios. Finally, in using AIs we could identify climate and hydrological conditions that could improve or worsen the growth of pasture species.

We conclude that an increase in mean temperature as expected during the 21st century may bring better conditions to the chosen pasture species on average by (i) increasing growing season length and (ii) increasing biomass. Uncertainty in future precipitation is seemingly less relevant for the growth in this water-abundant area, with likely no need of irrigation. An increased frequency of heat waves may occur, and a slight decrease in *Trisetum flavescens* biomass may be seen at the lowest altitudes (below 1100 m asl); however, this will be largely offset by an increased *Nardus stricta* yield at the highest altitudes.

Our results are of interest to scientists in the field of pasture/crop sciences willing to deepen into the potential impacts of climate change and to policy makers willing to explore strategies for adaptation. We further provided here possible hints for adaptation to breeders/farmers in Valtellina henceforth. Namely, one may suggest uplifting of pasture-related activity at higher altitudes than now, to concentrate investments in an area where potentially larger productivity will be attained, possibly aiding economic development in the valley.

Author Contributions: F.C. Contribution: literature review; conceptualization; methodology; software; data curation; formal analysis; writing—original draft preparation. D.B. Contribution: methodology; validation; software; resources; writing—review and editing; supervision; project administration. All authors have read and agreed to the published version of the manuscript.

Funding: This research received no external funding.

Data Availability Statement: Meteorological data, used for the study, are available in the ARPA Lombardia (Agenzia Regionale per la Protezione dell’Ambiente) repository: <https://www.arpalombardia.it/Pages/Meteorologia/Richiesta-dati-misurati.aspx>, accessed on 3 November 2022. The dataset of annual pasture productivity, used during the current study, is available in the ISTAT (Istituto Nazionale di Statistica) repository: <http://dati-censimentoagricoltura.istat.it/>, accessed on 3 November 2022. Data of local pasture biomass (at Alpe Boron) are included in this published article: Boschetti, M., Bocchi, S., & Brivio, P. A. (2007). Assessment of pasture production in the Italian Alps using spectrometric and remote sensing information. *Agriculture, ecosystems & environment*, 118(1–4), pp. 267–272. Data of local pasture biomass at Alpe Dosdè, used for the current study, are not publicly available, but they were given to the authors by Confalonieri, R., and Movedi, E. via personal communication and are available from the corresponding author on reasonable request and with the permission of Confalonieri, R., and Movedi, E.

Acknowledgments: This study is in fulfilment of IPCC-MOUPA (*Interdisciplinary Project for assessing current and expected Climate Change impacts on MOuntain PAstures*), a project of Università degli Studi di Milano and Politecnico di Milano, funded by Cariplo Foundation of Italy. F. Casale acknowledges support from the MOUPA project. S. Bocchi, R. Confalonieri, and E. Movedi of University Milano and the IPCC-MOUPA team are kindly acknowledged for fruitful discussion in the development of the present research. The authors acknowledge the support from the personnel of Climate-Lab (<https://www.climatelab.polimi.it/en/>, accessed on 3 November 2022), the Interdepartmental Laboratory on Climate Change at Politecnico di Milano. Eng. Giovanni Bombelli is kindly acknowledged for helping with the downscaling of IPCC scenarios.

Conflicts of Interest: The authors declare that they have no known competing financial interest or personal relationship that could have appeared to influence the work reported in this paper.

Appendix A. Poli-Hydro and Poli-Pasture Models

Appendix A.1. Poli-Hydro Model

The *Poli-Hydro* model is a spatially semi-distributed model, which applies mass conservation (continuity) equations to water content in the soil between two consequent time steps.

$$S^{t+\Delta t} = S^t + R + M_s - M_i - ET_{eff} - Q_g - Q_s \quad (A1)$$

where S is the soil water content (evaluated from land cover map using the SCS-CN method), R liquid rainfall, M_s snow melting, M_i ice melting (on ice covered areas), ET_{eff} actual evapotranspiration, Q_g groundwater discharge, and Q_s overland flow. The time step Δt was 1 day, and t is the considered day. Here, *Poli-Hydro* used cells of $1 \text{ km} \times 1 \text{ km}$ dimension.

Poli-Hydro is driven by meteorological data: temperature (T), (total) precipitation (P), and radiation (R_n). We used weather data of 15 ARPA Lombardia automatic weather stations for the period 2003–2019.

Snow and ice melting were calculated as follows:

$$M_{s,i} = DD_{s,i}(T_0 - T_t) \quad (A2)$$

where $DD_{s,i}$ [mm/°C/d] are the degree-day for snow and ice, T_0 is the threshold temperature for melting equal to $0 \text{ }^\circ\text{C}$, and T_t is the temperature of the day t .

The groundwater and overland discharges were calculated as:

$$Q_g = K \left(\frac{S}{S_{max}} \right)^k \quad (A3)$$

$$Q_s = S_{t+\Delta t} - S_{max} \quad \text{if } S_{t+\Delta t} > S_{max} \quad (A4)$$

$$Q_s = 0 \quad \text{if } S_{t+\Delta t} < S_{max}$$

with K [mm d⁻¹] saturated permeability and k [.] power exponent.

Potential evapotranspiration ET_{max} was calculated differently in pasture and nonpasture areas. In pasture lands, Priestley–Taylor’s formula (A.1) was used, and otherwise ET_{max} was calculated using Hargreaves’ formula (A.2):

$$ET_{max} = 1.26 \frac{\Delta}{\Delta + \gamma} \frac{R_n - G}{\lambda} \quad (A5)$$

$$ET_{max} = CR_a(T + 17.8)\sqrt{\Delta T} \quad (A6)$$

R_n is the net (at ground) radiation [MJ m⁻² d⁻¹], Δ is the slope of the pressure curve [kPa °C⁻¹], G is the heat flux from the soil [MJ m⁻² d⁻¹], γ is the psychrometric constant [kPa °C⁻¹], λ is the vaporization latent heat [MJ kg⁻¹]. C is a constant equal to 0.0023, R_a is the extraterrestrial solar radiation, T is the average daily temperature, and ΔT is the daily thermal excursion.

Then, the model estimated actual evapotranspiration ET_{eff} as the sum of effective evaporation from bare soil E_{ff} and effective transpiration T_{eff} . The latter was calculated here as a function of the plants’ properties:

$$T_{eff} = 86,400C / 1.5(\Psi_s - \Psi_x) \quad (A7)$$

where C [kg s m⁻⁴] is the root conductance, Ψ_s is soil water potential [J kg⁻¹] depending on water soil content S , and Ψ_x is the leaf water potential depending on plant roots development.

Appendix A.2. Poli-Pasture Model

The *Poli-Pasture* module runs jointly with *Poli-Hydro* model to calculate pasture species productivity.

Pasture lands in Valtellina were divided in two areas: above 2000 m asl (pasture zone HighAlt, high altitude) and below 2000 m asl (pasture zone LowAlt). Within the two zones, two species were identified through the more abundant. Above 2000 m asl, the most abundant species retrieved was *Nardus stricta*, while below 2000 m asl it was *Trisetum flavescens*.

Poli-Pasture was tuned using pasture yield statistics of ISTAT for the Sondrio province for the period 2006–2019 (control run period CR). In particular, specific (to area) production Y [t/ha] data were used. We also used an in situ estimation of specific annual production (of *Nardus stricta*) at high altitudes in the area of Valtellina valley. This came from the available literature for Alpe Boron during 2003 and 2004 [70] and from *Nardus stricta* biomass data collected in the Dosdè area during summer 2019 (two different sites, Dosdè 1, 2100 m asl, and Dosdè 2, 2500 m asl, Confalonieri R., personal communication, 2020), in fulfilment of the MOUPA project.

The *Poli-Pasture* model for each time step received from *Poli-Hydro* the daily value of soil water content S , to evaluate the growth of vegetal/agricultural species for the same time steps and cells. *Poli-Pasture* returned to *Poli-Hydro* a daily value of the leaf area index (LAI), used to assess correct daily evapotranspiration, fraction of soil with vegetal coverage, and soil water content (used for the vegetation growth).

Pasture species growth is based upon accumulation of thermal time stages (degree-days [$^{\circ}\text{C}$]). If the daily temperature is below base temperature T_{base} or above cutoff temperature T_{cutoff} , no thermal time is accumulated. The daily production of biomass for each species was estimated as the minimum value between water-dependent growth G_{TR} and solar radiation growth G_R :

$$G_{TR} = \frac{T_{eff} \cdot BTR}{VPD} \quad (\text{A8})$$

$$G_R = LtBc \cdot PAR \cdot f_{PAR} \cdot T_{lim} \quad (\text{A9})$$

with G_{TR} [$\text{kg m}^{-2} \text{d}^{-1}$] transpiration dependent biomass growth, T_{eff} [mm d^{-1}] actual transpiration, VPD [kPa] average vapor pressure deficit, BTR [kPa kg m^{-3}] biomass transpiration coefficient, G_R [$\text{kg m}^{-2} \text{d}^{-1}$] radiation-dependent biomass growth, $LtBc$ [kg MJ^{-1}] light-to-biomass conversion coefficient, PAR [$\text{MJ m}^{-2} \text{d}^{-1}$] photosynthetically active radiation, f_{PAR} [-] fraction of incident PAR intercepted by canopy, and T_{lim} temperature limitation factor [-]. These variables were calculated for each time step from the cumulated thermal time at that time step. The total annual production in a cell was calculated as the sum of peak biomass in each growth cycle.

Two kind of simulations were performed: with fixed and variable growing season for each species. In the first case, the growing season began on the 1st of April at low altitude and the 30th of April at high altitude. It ended on the 30th of September.

At low altitude, the *Trisetum flavescens* is harvested at maturity, while *Nardus stricta* at high altitudes is fed to animals upon flowering. After cut/feeding, growth started again, and the cycle was repeated until the end of the growing season.

In the second case, the growing season started when the mean temperature was higher than T_{base} (for each species) for 10 consecutive days, and it stopped when T was lower than the mean temperature of September 30th for 10 consecutive days.

References

1. Mazzocchi, C.; Ruggeri, G.; Sali, G. The role of tourists for pastures resilience and agriculture sustainability in the Alps: A multivariate analysis approach. In Proceedings of the 7th AIEAA Conference Evidence-based Policies to Face New Challenges for Agri-Food Systems, Conegliano, Italy, 14–15 June 2018.
2. Faccioni, G.; Sturaro, E.; Ramanzin, M.; Bernués, A. Socio-economic valuation of abandonment and intensification of Alpine agroecosystems and associated ecosystem services. *Land Use Policy* **2019**, *81*, 453–462. [[CrossRef](#)]

3. Hock, R.; Rasul, G.; Adler, C.; Cáceres, B.; Gruber, S.; Hirabayashi, Y.; Jackson, M.; Kääb, A.; Kang, S.; Kutuzov, S.; et al. Chapter 2: High Mountain Areas. IPCC Special Report on the Ocean and Cryosphere in a Changing Climate. *IPCC Spec. Rep. Ocean. Cryosphere A Chang. Clim.* **2019**, 131–202.
4. Böhm, R.; Auer, I.; Brunetti, M.; Maugeri, M.; Nanni, T.; Schöner, W. Regional temperature variability in the European Alps: 1760–1998 from homogenized instrumental time series. *Int. J. Climatol.* **2001**, *21*, 1779–1801. [[CrossRef](#)]
5. Brunetti, M.; Lentini, G.; Maugeri, M.; Nanni, T.; Simolo, C.; Spinoni, J. 1961–1990 high-resolution Northern and Central Italy monthly precipitation climatologies. *Adv. Sci. Res.* **2009**, *3*, 73–78. [[CrossRef](#)]
6. Dettinger, M.D.; Cayan, D.R. Large-scale atmospheric forcing of recent trends towards early snowmelt runoff in California. *J. Clim.* **1995**, 606–623. [[CrossRef](#)]
7. Cayan, D.R. Interannual climate variability and snowpack in the western United States. *J. Clim.* **1996**, 928–948. [[CrossRef](#)]
8. Haeberli, W.; Beniston, M. Climate change and its impacts on glaciers and permafrost in the Alps. *Ambio* **1998**, *27*, 258–265. [[CrossRef](#)]
9. Soncini, A.; Bocchiola, D. Assessment of future snowfall regimes within the Italian Alps using general circulation models. *Cold Reg. Sci. Technol.* **2011**, *68*, 113–123. [[CrossRef](#)]
10. Bocchiola, D.; Diolaiuti, G. Evidence of climate change within the Adamello Glacier of Italy. *Theor. Appl. Climatol.* **2010**, *100*, 351–369. [[CrossRef](#)]
11. Rohrer, M.B.; Braun, L.N.; Lang, H. Long-term records of snow cover water equivalent in the Swiss Alps 1. Analysis. *Nord. Hydrol.* **1994**, *25*, 65–78. [[CrossRef](#)]
12. Beniston, M.; Diaz, H.F.; Bradley, R.S. Climatic change at high elevation sites: An overview. *Clim. Chang.* **1997**, *36*, 233–251. [[CrossRef](#)]
13. Braun, L.N.; Weber, M.; Schulz, M. Consequences of climate change for runoff from Alpine regions. *Ann. Glaciol.* **2000**, *31*. [[CrossRef](#)]
14. Laternser, M.; Schneebeli, M. Long-term snow climate trends of the Swiss Alps (1931–99). *Int. J. Climatol.* **2003**, *23*, 733–750. [[CrossRef](#)]
15. Liu, J.; Hayakawa, N.; Lu, M.; Dong, S.; Yuan, J. Hydrological and geocryological response of winter streamflow to climate warming in Northeast China. *Cold Reg. Sci. Technol.* **2003**, *37*, 15–24. [[CrossRef](#)]
16. Bavay, M.; Lehning, M.; Jonas, T.; Lowe, H. Simulations of future snow cover and discharge in Alpine headwater catchments. *Hydrol. Process.* **2009**, *23*, 95–108. [[CrossRef](#)]
17. Groppelli, B.; Soncini, A.; Bocchiola, D.; Rosso, R. Evaluation of future hydrological cycle under climate change scenarios in a mesoscale Alpine watershed of Italy. *Nat. Hazards Earth Syst. Sci.* **2011**, *11*, 1769–1785. [[CrossRef](#)]
18. Confortola, G.; Soncini, A.; Bocchiola, D. Climate change will affect hydrological regimes in the Alps. *Rev. Géographie Alp.* **2014**, *101*. [[CrossRef](#)]
19. Van Der Wal, R.; Madan, N.; Van Lieshout, S.; Dormann, C.; Langvatn, R.; Albon, S.D. Trading forage quality for quantity? Plant phenology and patch choice by Svalbard reindeer. *Oecologia* **2000**, *123*, 108–115. [[CrossRef](#)]
20. Zeeman, M.J.; Mauder, M.; Steinbrecher, R.; Heidbach, K.; Eckart, E.; Schmid, H.P. Reduced snow cover affects productivity of upland temperate grasslands. *Agric. For. Meteorol.* **2017**, *232*, 514–526. [[CrossRef](#)]
21. Huber, R.; Briner, S.; Peringer, A.; Lauber, S.; Seidl, R.; Widmer, A.; Gillet, F.; Buttler, A.; Le, Q.B.; Hirschi, C. Modeling social-ecological feedback effects in the implementation of payments for environmental services in pasture-woodlands. *Ecol. Soc.* **2013**, *18*, 41. [[CrossRef](#)]
22. Briner, S.; Elkin, C.; Huber, R. Evaluating the relative impact of climate and economic changes on forest and agricultural ecosystem services in mountain regions. *J. Environ. Manag.* **2013**, *129*, 414–422. [[CrossRef](#)] [[PubMed](#)]
23. Dibari, C.; Costafreda-Aumedes, S.; Argenti, G.; Bindi, M.; Carotenuto, F.; Moriondo, M.; Padovan, G.; Pardini, A.; Staglianò, N.; Vagnoli, C.; et al. Expected changes to alpine pastures in extent and composition under future climate conditions. *Agronomy* **2020**, *10*, 926. [[CrossRef](#)]
24. Addimando, N.; Nana, E.; Bocchiola, D. Modeling pasture dynamics in a Mediterranean environment: Case study in Sardinia, Italy. *J. Irrig. Drain. Eng.* **2015**, *141*. [[CrossRef](#)]
25. Confalonieri, R. CoSMo: A simple approach for reproducing plant community dynamics using a single instance of generic crop simulators. *Ecol. Model.* **2014**, *286*, 1–10. [[CrossRef](#)]
26. Bocchiola, D.; Soncini, A. Pasture Modelling in Mountain Areas: The Case of Italian Alps, and Pakistani Karakoram. *Agric. Res. Technol. Open Access J.* **2017**, *8*, 1–8. [[CrossRef](#)]
27. Tubiello, F.N.; Soussana, J.F.; Howden, S.M. Crop and pasture response to climate change. *Proc. Natl. Acad. Sci. USA* **2007**, *104*, 19686–19690. [[CrossRef](#)]
28. Fan, J.W.; Shao, Q.Q.; Liu, J.Y.; Wang, J.B.; Harris, W.; Chen, Z.Q.; Zhong, H.P.; Xu, X.L.; Liu, R.G. Assessment of effects of climate change and grazing activity on grassland yield in the Three Rivers Headwaters Region of Qinghai-Tibet Plateau, China. *Environ. Monit. Assess.* **2010**, *170*, 571–584. [[CrossRef](#)]
29. Fuso, F.; Casale, F.; Giudici, F.; Bocchiola, D. Future Hydrology of the Cryospheric Driven Lake Como Catchment in Italy under Climate Change Scenarios. *Climate* **2021**, *9*, 8. [[CrossRef](#)]

30. Stöckle, C.O.; Nelson, R.; Donatelli, M.; Yan, Y.; Ferrer, F.; Van Evert, F.; Mccool, D.; Martin, S.; Mulla, D.; Bechini, L.; et al. *Cropping Systems Simulation Model User's Manual*; Washington State University Biological System Engineering Department: Washington, DC, USA, 1994.
31. Dale, V.H.; Polasky, S. Measures of the effects of agricultural practices on ecosystem services. *Ecol. Econ.* **2007**, *64*, 286–296. [[CrossRef](#)]
32. Briner, S.; Elkin, C.; Huber, R.; Grêt-Regamey, A. Assessing the impacts of economic and climate changes on land-use in mountain regions: A spatial dynamic modeling approach. *Agric. Ecosyst. Environ.* **2012**, *149*, 50–63. [[CrossRef](#)]
33. Nana, E.; Corbari, C.; Bocchiola, D. A model for crop yield and water footprint assessment: Study of maize in the Po valley. *Agric. Syst.* **2014**, *127*, 139–149. [[CrossRef](#)]
34. Bocchiola, D. Impact of potential climate change on crop yield and water footprint of rice in the Po valley of Italy. *Agric. Syst.* **2015**, *139*, 223–237. [[CrossRef](#)]
35. Egarter Vigl, L.; Tasser, E.; Schirpke, U.; Tappeiner, U. Using land use/land cover trajectories to uncover ecosystem service patterns across the Alps. *Reg. Environ. Change* **2017**, *17*, 2237–2250. [[CrossRef](#)]
36. Life Pastoralp. *Pastures Vulnerability and Adaptation Strategies to Climate Change Impacts in the Alps Deliverable C. 1 Report on Future Climate Scenarios for the Two Study Areas*; Life Pastoralp: Florence, Italy, 2019.
37. Nobakht, M.; Beavis, P.; O'Hara, S.; Hutjes, R.; Supit, I. *Agroclimatic Indicators Product User Guide and Specification*; ECMWF Copernicus: Bologna, Italy, 2019.
38. Arnell, N.W.; Freeman, A. The effect of climate change on agro-climatic indicators in the UK. *Clim. Change* **2021**, *165*, 1–26. [[CrossRef](#)]
39. Rivington, M.; Matthews, K.B.; Buchan, K.; Miller, D.G.; Bellocchi, G.; Russell, G. Climate change impacts and adaptation scope for agriculture indicated by agro-meteorological metrics. *Agric. Syst.* **2013**, *114*, 15–31. [[CrossRef](#)]
40. Rötter, R.P.; Höhn, J.; Trnka, M.; Fronzek, S.; Carter, T.R.; Kahiluoto, H. Modelling shifts in agroclimate and crop cultivar response under climate change. *Ecol. Evol.* **2013**, *3*, 4197–4214. [[CrossRef](#)]
41. Thornley, J.H.M. *Grassland Dynamics: An Ecosystem Simulation Model*; CAB International: Wallingford, UK, 1998.
42. Johnson, I.R. *Biophysical Pasture Model Documentation Model Documentation for DairyMod, EcoMod and the SGS Pasture Model*; IMJ Consultants: Dorrigo, NSW, Australia, 2008.
43. Peel, M.C.; Finlayson, B.L.; McMahon, T.A. Updated world map of the Köppen-Geiger climate classification. *Hydrol. Earth Syst. Sci.* **2007**, *11*, 1633–1644. [[CrossRef](#)]
44. Bocchiola, D.; Mihalcea, C.; Diolaiuti, G.; Mosconi, B.; Smiraglia, C.; Rosso, R. Flow prediction in high altitude ungauged catchments: A case study in the Italian Alps (Pantano Basin, Adamello Group). *Adv. Water Resour.* **2010**, *33*, 1224–1234. [[CrossRef](#)]
45. Gusmeroli, F.; Corti, M.; Orlandi, D.; Pasut, D.; Bassignana, M.; Fausto, D.; Fondazioni, G.; Superiori, S. Produzione E Prerogative Qualitative Dei Pascoli Alpini: Riflessi Sul Comportamento Al Pascolo E L' Ingestione. In Proceedings of the Convegno SoZooAlp L'Alimentazione della Vacca da Latte al Pascolo: Riflessi Zootecnici, Agroambientali e Sulla Tipicità delle Produzioni, Bagni Masino (SO), Sondrio, Italy, 1–3 July 2004; pp. 7–28.
46. Gusmeroli, F. Il piano di pascolamento: Strumento fondamentale per una corretta gestione del pascolo. In Proceedings of the Convegno SoZooAlp Il Sistema delle Malghe Alpine: Aspetti Agro-Zootecnici, Paesaggistici e Turistici, Piancavallo (PN), Pordenone, Italy, 5–6 September 2003; pp. 27–41.
47. Barcella, M.; Gusmeroli, F. *La Gestione delle Superfici Pascolive. Linee Guida per la Gestione dei Pascoli a Nardo*; Fondazione Cariplo: Milan, Italy, 2018.
48. Aili, T.; Soncini, A.; Bianchi, A.; Diolaiuti, G.; D'Agata, C.; Bocchiola, D. Assessing water resources under climate change in high-altitude catchments: A methodology and an application in the Italian Alps. *Theor. Appl. Climatol.* **2019**, *135*, 135–156. [[CrossRef](#)]
49. Bocchiola, D.; Diolaiuti, G.; Soncini, A.; Mihalcea, C.; D'Agata, C.; Mayer, C.; Lambrecht, A.; Rosso, R.; Smiraglia, C. Prediction of future hydrological regimes in poorly gauged high altitude basins: The case study of the upper Indus, Pakistan. *Hydrol. Earth Syst. Sci.* **2011**, *15*, 2059–2075. [[CrossRef](#)]
50. Bocchiola, D.; Soncini, A.; Senese, A.; Diolaiuti, G. Modelling hydrological components of the Rio Maipo of Chile, and their prospective evolution under climate change. *Climate* **2018**, *6*, 57. [[CrossRef](#)]
51. Bocchiola, D.; Brunetti, L.; Soncini, A.; Polinelli, F.; Gianinetto, M. Impact of climate change on agricultural productivity and food security in the Himalayas: A case study in Nepal. *Agric. Syst.* **2019**, *171*, 113–125. [[CrossRef](#)]
52. Stöckle, C.O.; Nelson, R.; Mccool, D. Cropping Systems Simulation Model User ' s Manual CropSyst Preface. *Simulation* **2001**, 235.
53. Ziliotto, U.; Scotton, M.; Da Ronch, F. I pascoli alpini: Aspetti ecologici e vegetazionali. In Proceedings of the Convegno SoZooAlp Il Sistema delle Malghe Alpine: Aspetti Agro-Zootecnici, Paesaggistici e Turistici, Piancavallo (PN), Pordenone, Italy, 5–6 September 2003; pp. 11–26.
54. Erfini, R. *Analisi dello stato gestionale dei prati della Val Grosina e delle potenzialità foraggiere del Comune di Grosio*. Master's Thesis, University of Milan, Milan, Italy, 2017.
55. Bocchiola, D.; Rosso, R. The distribution of daily snow water equivalent in the central Italian Alps. *Adv. Water Resour.* **2007**, *30*, 135–147. [[CrossRef](#)]
56. Valt, M.; Chiambretti, I.; Dellavedova, P. Fresh snow density on the Italian Alps. In Proceedings of the EGU General Assembly, Vienna, Austria, 27 April–2 May 2014; Volume 16.

57. Soncini, A.; Bocchiola, D.; Azzoni, R.S.; Diolaiuti, G. A methodology for monitoring and modeling of high altitude Alpine catchments. *Prog. Phys. Geogr.* **2017**, *41*, 393–420. [[CrossRef](#)]
58. Mishra, S.K.; Singh, V.P. SCS-CN Method. In Soil Conservation Service Curve Number (SCS-CN) Methodology. *Water Sci. Technol. Libr.* **2003**, *42*, 84–146. [[CrossRef](#)]
59. Saxton, K.E.; Rawls, W.J.; Romberger, J.S.; Papendick, R.I. Estimating soil water characteristics-hydraulic conductivity. *Soil Sci. Soc. Am. J.* **1986**, *5*, 1031–1036. [[CrossRef](#)]
60. Bombelli, G.M.; Soncini, A.; Bianchi, A.; Bocchiola, D. Potentially modified hydropower production under climate change in the Italian Alps. *Hydrol. Process.* **2019**, *33*, 2355–2372. [[CrossRef](#)]
61. Angus, J.F.; Cunningham, R.B.; Moncur, M.W.; Mackenzie, D.H. Phasic development in field crops I. Thermal response in the seedling phase. *Field Crops Res.* **1980**. [[CrossRef](#)]
62. Movedi, E.; Bellocchi, G.; Argenti, G.; Paleari, L.; Vesely, F.; Staglianò, N.; Dibari, C.; Confalonieri, R. Development of generic crop models for simulation of multi-species plant communities in mown grasslands. *Ecol. Model.* **2019**, *401*, 111–128. [[CrossRef](#)]
63. Moreira Marcelo, Z.; Sternberg Leonel da, S.L.; Nepstad Daniel, C. Vertical patterns of soil water uptake by plants in a primary forest and an abandoned pasture in the eastern Amazon: An isotopic approach. *Plant Soil* **2000**, *222*, 95–107.
64. Confalonieri, R.; Acutis, M.; Bellocchi, G.; Donatelli, M. Multi-metric evaluation of the models WARM, CropSyst, and WOFOST for rice. *Ecol. Model.* **2009**, *220*, 1395–1410. [[CrossRef](#)]
65. Gusmeroli, F. (Ed.) Il paesaggio vegetale alpino. In *Prati e Pascoli e Paesaggio Alpino*; SoZooAlp Editore: San Michele all'Adige, Italy, 2012; pp. 131–179.
66. De Silva, M.S.; Nachabe, M.H.; Šimůnek, J.; Carnahan, R. Simulating root water uptake from a heterogeneous vegetative cover. *J. Irrig. Drain. Eng.* **2008**, *134*, 167–174. [[CrossRef](#)]
67. Monks, D.; SadatAsilan, K.; Moot, D. Cardinal temperatures and thermal time requirements for germination of annual and perennial temperate pasture species. In Proceedings of the 38th Agronomy Society Conference, Lincoln, New Zealand, 4–5 May 2009. [[CrossRef](#)]
68. Moot, D.J.; Scott, W.R.; Roy, A.M.; Nicholls, A.C. Base temperature and thermal time requirements for germination and emergence of temperate pasture species. *N. Z. J. Agric. Res.* **2000**, *43*, 15–25. [[CrossRef](#)]
69. Boschetti, M.; Bocchi, S.; Brivio, P.A. Assessment of pasture production in the Italian Alps using spectrometric and remote sensing information. *Agric. Ecosyst. Environ.* **2007**, *118*, 267–272. [[CrossRef](#)]
70. Groppelli, B.; Bocchiola, D.; Rosso, R. Spatial downscaling of precipitation from GCMs for climate change projections using random cascades: A case study in Italy. *Water Resour. Res.* **2011**, *47*. [[CrossRef](#)]
71. Stocker, T.F.; Qin, D.; Plattner, G.-K.; Tignor, M.M.B.; Allen, S.K.; Boschung, J.; Nauels, A.; Xia, Y.; Bex, V.; Midgley, P.M.; et al. *Climate Change 2013. The Physical Science Basis. Working Group I Contribution to the Fifth Assessment Report of the Intergovernmental Panel on Climate Change*; Cambridge University Press: Cambridge, UK, 2013.
72. Stevens, B.; Giorgetta, M.; Esch, M.; Mauritsen, T.; Crueger, T.; Rast, S.; Salzmann, M.; Schmidt, H.; Bader, J.; Block, K.; et al. Atmospheric component of the MPI-M earth system model: ECHAM6. *J. Adv. Model. Earth Syst.* **2013**, *5*, 146–172. [[CrossRef](#)]
73. Gent, P.R.; Danabasoglu, G.; Donner, L.J.; Holland, M.M.; Hunke, E.C.; Jayne, S.R.; Lawrence, D.M.; Neale, R.B.; Rasch, P.J.; Vertenstein, M.; et al. The community climate system model version 4. *J. Clim.* **2011**, *24*, 4973–4991. [[CrossRef](#)]
74. Hazeleger, W.; Wang, X.; Severijns, C.; Ștefănescu, S.; Bintanja, R.; Sterl, A.; Wyser, K.; Semmler, T.; Yang, S.; van den Hurk, B.; et al. EC-Earth V2.2: Description and validation of a new seamless earth system prediction model. *Clim. Dyn.* **2012**, *39*, 2611–2629. [[CrossRef](#)]
75. Eyring, V.; Bony, S.; Meehl, G.A.; Senior, C.; Stevens, B.; Stouffer, R.J.; Taylor, K.E. Overview of the Coupled Model Intercomparison Project Phase 6 (CMIP6) experimental design and organisation. *Geosci. Model Dev. Discuss.* **2015**, *8*, 10539–10583. [[CrossRef](#)]
76. Hartung, K.; Svensson, G.; Struthers, H.; Deppenmeier, A.L.; Hazeleger, W. An EC-Earth coupled atmosphere-ocean single-column model (AOSCM.v1-EC-Earth3) for studying coupled marine and polar processes. *Geosci. Model Dev.* **2018**, *11*, 4117–4137. [[CrossRef](#)]
77. Mauritsen, T.; Bader, J.; Becker, T.; Behrens, J.; Bittner, M.; Brokopf, R.; Brovkin, V.; Claussen, M.; Crueger, T.; Esch, M.; et al. Developments in the MPI-M Earth System Model version 1.2 (MPI-ESM1.2) and Its Response to Increasing CO₂. *J. Adv. Model. Earth Syst.* **2019**, *11*, 998–1038. [[CrossRef](#)]
78. Danabasoglu, G.; Lamarque, J.F.; Bacmeister, J.; Bailey, D.A.; DuVivier, A.K.; Edwards, J.; Emmons, L.K.; Fasullo, J.; Garcia, R.; Gettelman, A.; et al. The Community Earth System Model Version 2 (CESM2). *J. Adv. Model. Earth Syst.* **2020**, *12*. [[CrossRef](#)]
79. Casale, F.; Fuso, F.; Giuliani, M.; Castelletti, A.; Bocchiola, D. Exploring future vulnerabilities of subalpine Italian regulated lakes under different climate scenarios: Bottom-up vs top-down and CMIP5 vs CMIP6. *J. Hydrol. Reg. Stud.* **2021**, *38*, 100973. [[CrossRef](#)]
80. Bocchiola, D.; Nana, E.; Soncini, A. Impact of climate change scenarios on crop yield and water footprint of maize in the Po valley of Italy. *Agric. Water Manag.* **2013**, *116*, 50–61. [[CrossRef](#)]
81. Kuczera, G.; Parent, E. Monte Carlo assessment of parameter uncertainty in conceptual catchment models: The Metropolis algorithm. *J. Hydrol.* **1998**, *211*, 69–85. [[CrossRef](#)]
82. Johnson, I.R.; Chapman, B., D.F.; Snow, V.O.; Eckard, R.J.; Parsons, A.J.; Lambert, M.G.; Cullen, B.R. DairyMod and EcoMod: Biophysical pasture-simulation models for Australia and New Zealand. *Aust. J. Exp. Agric.* **2008**, *48*, 621–631. [[CrossRef](#)]
83. McCall, D.G.; Bishop-Hurley, G.J. A pasture growth model for use in a whole-farm dairy production model. *Agric. Syst.* **2003**, *76*, 1183–1205. [[CrossRef](#)]

84. Insua, J.R.; Utsumi, S.A.; Basso, B. Assessing and Modeling Pasture Growth under Different Nitrogen Fertilizer and Defoliation Rates in Argentina and the United States. *Agron. J.* **2019**, *111*, 702–713. [[CrossRef](#)]
85. Insua, J.R.; Utsumi, S.A.; Basso, B. Estimation of spatial and temporal variability of pasture growth and digestibility in grazing rotations coupling unmanned aerial vehicle (UAV) with crop simulation models. *PLoS ONE* **2019**, *14*, e0212773. [[CrossRef](#)]
86. Liu, L.; Basso, B. Spatial evaluation of switchgrass productivity under historical and future climate scenarios in Michigan. *GCB Bioenergy* **2017**, *9*, 1320–1332. [[CrossRef](#)]
87. Ruelle, E.; Hennessy, D.; Delaby, L. Development of the Moorepark St Gilles grass growth model (MoSt GG model): A predictive model for grass growth for pasture based systems. *Eur. J. Agron.* **2018**, *99*, 80–91. [[CrossRef](#)]
88. Cho, M.A.; Skidmore, A.; Corsi, F.; van Wieren, S.E.; Sobhan, I. Estimation of green grass/herb biomass from airborne hyper-spectral imagery using spectral indices and partial least squares regression. *Int. J. Appl. Earth Obs. Geoinf.* **2007**, *9*, 414–424. [[CrossRef](#)]
89. Bloor, J.M.G.; Pichon, P.; Falcimagne, R.; Leadley, P.; Soussana, J.-F. Effects of Warming, Summer Drought, and CO₂ Enrichment on Aboveground Biomass Production, Flowering Phenology, and Community Structure in an Upland Grassland Ecosystem. *Ecosystem* **2010**, *13*, 888–900. [[CrossRef](#)]
90. Niedrist, G.; Tasser, E.; Bertoldi, G.; Della Chiesa, S.; Obojes, N.; Egarter-Vigl, L.; Tappeiner, U. Down to future: Transplanted mountain meadows react with increasing phytomass or shifting species composition. *Flora Morphol. Distrib. Funct. Ecol. Plants* **2016**, *224*, 172–182. [[CrossRef](#)]
91. Nagase, A.; Dunnett, N. Drought tolerance in different vegetation types for extensive green roofs: Effects of watering and diversity. *Landsc. Urban Plan.* **2010**, *97*, 318–327. [[CrossRef](#)]
92. Lamprecht, A.; Semenchuk, P.R.; Steinbauer, K.; Winkler, M.; Pauli, H. Climate change leads to accelerated transformation of high-elevation vegetation in the central Alps. *New Phytol.* **2018**, *220*, 447–459. [[CrossRef](#)] [[PubMed](#)]
93. Xu, C.; Liu, H.; Williams, A.P.; Yin, Y.; Wu, X. Trends toward an earlier peak of the growing season in Northern Hemisphere mid-latitudes. *Glob. Change Biol.* **2016**, *22*. [[CrossRef](#)] [[PubMed](#)]
94. Carlson, B.Z.; Corona, M.C.; Dentant, C.; Bonet, R.; Thuiller, W.; Choler, P. Observed long-term greening of alpine vegetation—A case study in the French Alps. *Environ. Res. Lett.* **2017**, *12*, 114006. [[CrossRef](#)]
95. Mastrotheodoros, T.; Pappas, C.; Molnar, P.; Burlando, P.; Hadjidoukas, P.; Fatichi, S. Ecohydrological dynamics in the Alps: Insights from a modelling analysis of the spatial variability. *Ecohydrology* **2019**, *12*, e2054. [[CrossRef](#)]
96. Saito, M.; Kato, T.; Tang, Y. Temperature controls ecosystem CO₂ exchange of an alpine meadow on the northeastern Tibetan Plateau. *Glob. Change Biol.* **2009**. [[CrossRef](#)]
97. Targetti, S.; Staglianò, N.; Messeri, A.; Argenti, G. A state-and-transition approach to alpine grasslands under abandonment. *IForest* **2010**, *3*, 44–51. [[CrossRef](#)]
98. Argenti, G.; Lombardi, G. The pasture-type approach for mountain pasture description and management. *Ital. J. Agron.* **2012**, *7*, 293–299. [[CrossRef](#)]
99. D’ottavio, P.; Ziliotto, U. Effect of different management on the production characteristics of mountain permanent meadows. *Ital. J. Anim. Sci.* **2003**. [[CrossRef](#)]
100. Haldemann, C.; Fuhrer, J. Interactive Effects of CO₂ and O₃ on the Growth of *Trisetum flavescens* and *Trifolium pratense* Grown in Monoculture or a Bi-Species Mixture. *J. Crop Improv.* **2005**, *13*, 275–289. [[CrossRef](#)]
101. Beukes, P.C.; Palliser, C.C.; Macdonald, K.A.; Lancaster, J.A.S.; Levy, G.; Thorrold, B.S.; Wastney, M.E. Evaluation of a Whole-Farm Model for Pasture-Based Dairy Systems. *J. Dairy Sci.* **2008**, *91*, 2353–2360. [[CrossRef](#)]